NASA

FINAL REPORT

THEORETICAL STUDY OF THE MECHANISMS OF FATIGUE IN PHOTOMULTIPLIERS

By Ramon U. Martinelli and George A. Morton

Prepared under Contract No. NAS 1-8169 by

RCA CORPORATION
Electronic Components
Conversion Devices Laboratory
David Sarnoff Research Center
Princeton, New Jersey 08540

for

NATIONAL AERONAUTICS AND SPACE ADMINISTRATION

TABLE OF CONTENTS

SUMMARY

The decrease in secondary emission ratio as a function of time and primary beam current density has been investigated for the Cu-Be and Ag-Mg dynodes of conventional photomultipliers and for the high-gain GaP dynodes.

After an initial decay proportional to the charge density ($\int idt$), the rate of decrease is approximately proportional to the logarithm of the incident charge density. From the photoelectric and gain behavior, it was concluded that both the escape depth and the escape probability are decreased by fatigue of GaP high-gain secondary emitters. Circuits for overcoming the effects of fatigue by photon counting and voltage feedback with a calibrated light source are described for high first-stage gain photomultipliers used for photometry.

I. INTRODUCTION

This report covers the second phase of a research program investigating fatigue in photomultipliers. The first portion of this phase dealt, as did Phase I, with fatigue in conventional photomultipliers with copper beryllium or silver magnesium dynodes. The second, and most important, part considers multipliers with GaP dynodes.[1] These multipliers, developed in this Laboratory and only recently having become a commercial item, appear to be at least as stable as those with the more conventional dynodes. The excellent pulse height resolution capabilities of tubes using these dynodes together with their greater time resolution potential (because of higher interstage voltages and lower secondary electron initial velocities) make it probable that the new tubes will replace conventional photomultipliers in most applications.[2]

Fatigue is the term applied to a certain type of instability in photomultipliers which leads to a gradual decrease in gain as the tube is operated at fairly high currents. In general, the tube will recover some of its lost gain when the stimulating light is removed from the cathode. There are other types of instabilities which can cause gain changes. Usually these other effects, which may cause an increase or decrease in gain with tube operation, are much more rapid and are therefore easily distinguished from true fatigue. Some of the causes of the second type of instabilities are the effects of insulated surface charging on multiplier gain and improper cesiation (over-cesiation) of dynode surfaces.

The problem of multiplier fatigue is one which has been recognized for a long time.[3,4] So far, no adequate explanation or cure has been suggested for the phenomenon. It is a difficult one to study because so little is known about the physics and chemistry of dynodes. Furthermore, and perhaps because of the above, it is very difficult to obtain reproducible results.

There is a greater probability of the problem being solved with the GaP dynodes because the solid state physics of these dynodes is better understood. However, even with this material, a quantitative study is difficult and time-consuming.

During the first phase of the research, a measuring unit was designed and built which held the test illumination on the cathode constant and permitted monitoring and recording the gain from three points along the dynode chain of the multiplier. A GaAsP light source pulsed 2000 times a second served as the calibrating light. Ninety-five percent of this light was directed onto the multiplier being tested; the rest

went to a phototube and feedback control circuit to hold the light from the source constant.

The pulses from the power source supplying the light were used to actuate phase-sensitive detectors on the three measuring leads. The output from the measuring circuits were recorded on a time-sharing Leeds and Northrup recorder.

The fatiguing light was a separate incandescent light source which gave a dc photocurrent from the multiplier photocathode. The fatiguing light source was unregulated, and the fatiguing current was measured with a dc meter in the anode circuit.

For relatively short fatigue runs of one or a few hours, the recorder was run continuously. For longer runs, the various currents were sampled and recorded at 15 minute intervals.

A block diagram of the unit is shown in Fig. 1. Fig. 2 illustrates the current flow in a multiplier. With the measuring leads at the anode, dynode n (D_n), and dynode n-1 (D_{n-1}), the gains δ_n and δ_{n-1} can be calculated as follows:

$$\delta_n = \frac{i_A}{i_A - i_{D_n}} = \frac{i_A}{i_{D_{n-1}}} \times \frac{i_{D_{n-1}}}{i_A - i_{D_n}}$$

$$\delta_{n-1} = \frac{i_A - i_{D_n}}{i_A - i_{D_n} - i_{D_{n-1}}}$$

The system was used to measure a number of multipliers with CuBe and AgMg dyndoes. Most of these were commercial phototubes, but several special experimental tubes were explored.

It was found that a number of multipliers showed a rapid change of gain when first operated. This could be either an increase or decrease - more frequently the latter. Experiments with a number of different types of tubes, including one with no insulating supports at the ends of the dynodes, showed this change to be due to insulator charging and not to fatigue proper.

It was found that many multipliers showed a decrease of gain which over long periods was approximately proportional to the logarithm of the operating time. Furthermore, there appeared to exist a form of reciprocity, so that the decay in gain was a function of the product of current and time (charge) striking the surface. Since there was also a recovery

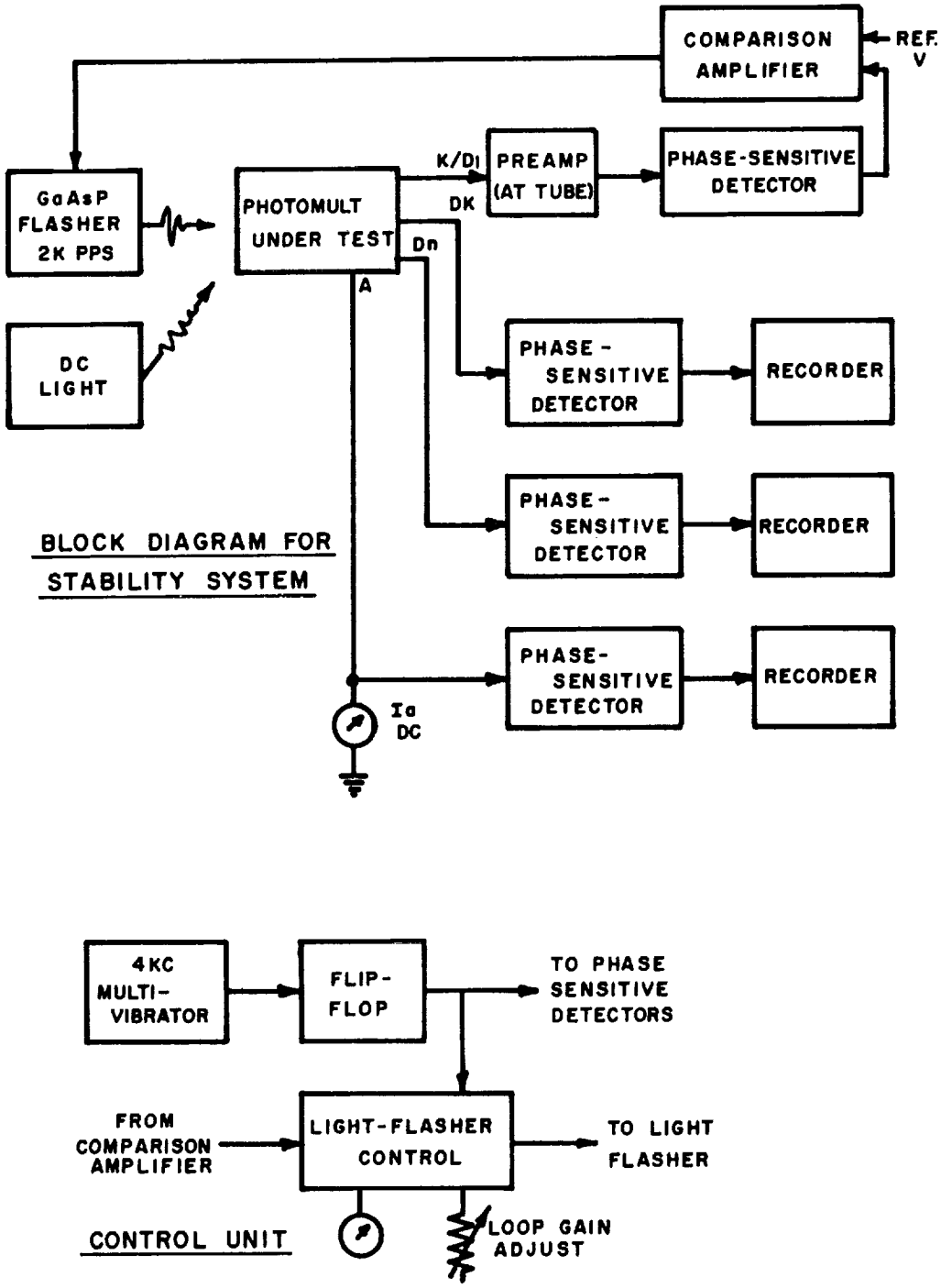

FIG 1. FATIGUE TEST UNIT

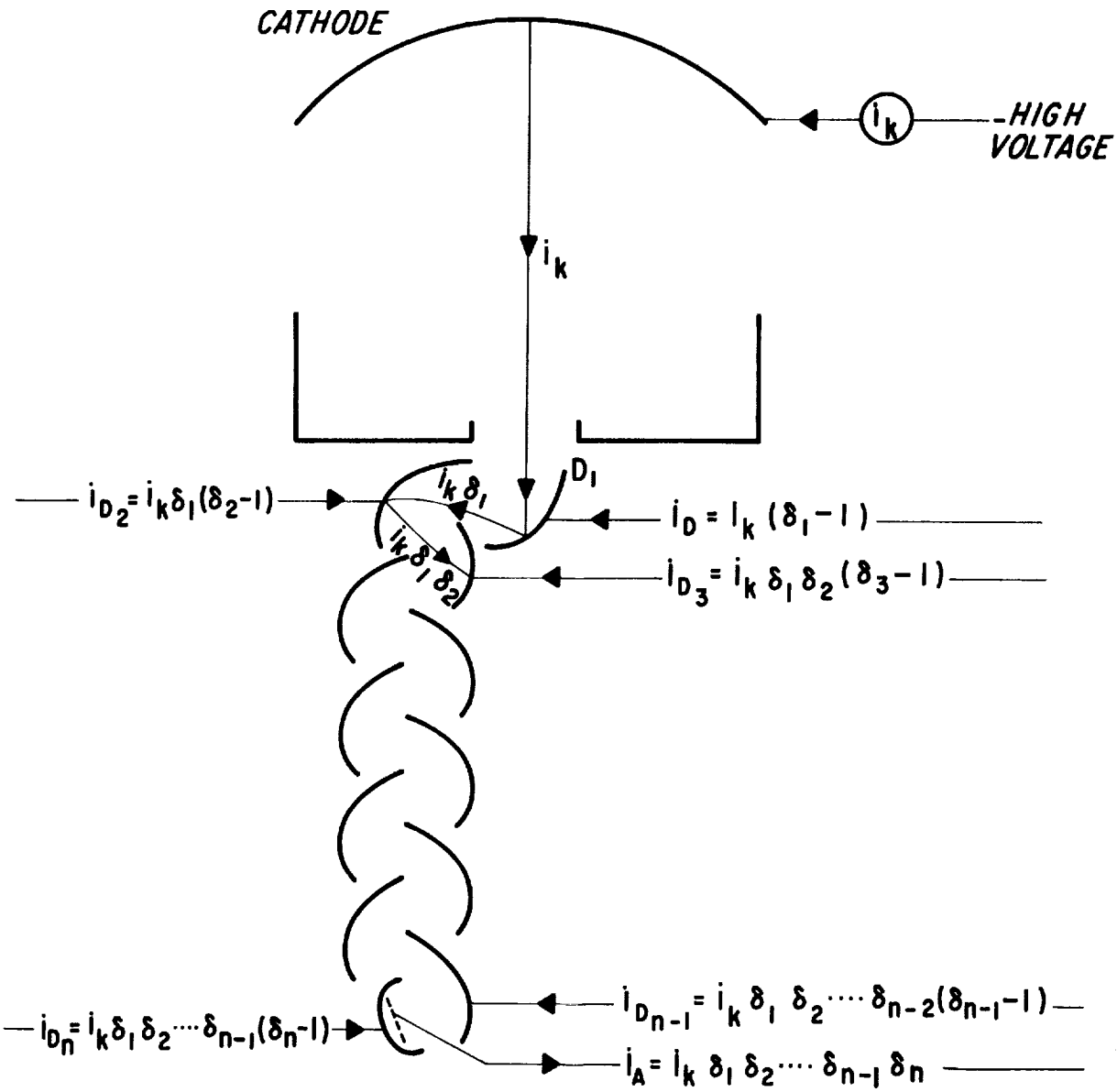

FIG. 2. CURRENT FLOW IN PHOTOMULTIPLIERS

or healing process which went on irrespective of whether a surface was being bombarded or not, both the logarithmic relation with charge and the reciprocity breakdown at low currents and long times.

The relationships noted are not laws and have not been proven. However, something close to them is not unexpected and the relationship ΔG vs ℓn (charge) makes a convenient way of expressing measured results.

Many exceptions have been observed to the above. For example, in some tubes the gain is observed to drop in proportion to the logarithm of time with one constant of proportionality for a certain length of time, then change the constant of proportionality for no apparent reason.

The second phase of the research attempted to relate fatigue with the mechanism of secondary emission. As will be shown in greater detail in the discussion of the physics of secondary emission, three processes are involved; namely, (1) the excitation of an electron from the valence band into a more energetic state (i.e., to becoming a "hot electron" with conventional secondary emitters, or into the conduction band for GaP), (2) the transport of the excited electron to the vacuum-secondary emitter interface, and (3) the escape of the electron from the emitting surface. It can be assumed that the excitation process is probably not affected by the bombardment of the material by the primary electrons. Either or both of the other two steps in the emission process may be affected. In determining a method of overcoming fatigue, it would be very helpful to know the extent to which each process was involved.

By using a range of bombarding electron velocities and by observing the effect of fatigue in the photoelectric response of the material, it should be possible to separate the two processes. While a start was made on doing this, time did not permit completing the necessary research.

II. THE PHYSICS OF SECONDARY EMISSION[5,6]

The following discussion proceeds along lines similar to that given in the Final Report of the first phase of this research. However, since it is quite essential to any long range consideration of multiplier fatigue, any repetition there may be is deemed warranted.

As has been mentioned, secondary emission is a three-step process. The energy of the incident primary is given to a number of electrons in the valence band, giving them energy enough so that they are excited above the bottom of the conduction band. The electrons move through the material to the surface. If, when they reach the surface, they have energy enough to surmount the energy barrier between the vacuum and the material, they can escape as secondary electrons.

Either of two rather fundamentally different conditions may exist at the surface. The potential of the vacuum may be above the bottom of the conduction band or it may be below it. The former is the situation with conventional secondary emitters. When it obtains, the electrons, in order to escape, must be "hot" electrons. Since the rate of loss of energy of electrons above the conduction band is very high, these "hot" electrons must come from very close to the surface, i.e., 50 or 100 Å. One of the consequences of this is that a very energetic primary will penetrate so far into the material that electrons excited at the end of its range cannot escape. Therefore the maximum yield occurs at relatively low voltage, i.e., 500 to 1000 volts.

The vacuum potential is below the bottom of the conduction band in the new secondary emitters such as cesium activated gallium phosphide.[7] This is possible because of band bending due to charges in the material. For example, with GaP, the bulk material is made strongly p-type by the use of a zinc impurity, and the surface is treated with cesium which permits a charge rearrangement at or near the surface that brings the vacuum level to about 1.4 eV above the Fermi level. Because of the p-type doping, the Fermi level of the bulk is essentially at the valence band or 2.3 eV below the bottom of the conduction band. There is an effective negative affinity of about 0.9 eV. A possible configuration is illustrated in Fig. 3, showing a sharply bent conduction band due to charge rearrangement.

As a consequence, electrons which are thermally diffusing in the material can escape when they approach the surface. Where the lifetime of a "hot" electron in a conventional emitter is on the order of 10^{-13} sec and the escape depth only 50 to 100 Å, the lifetime of a thermally diffusing

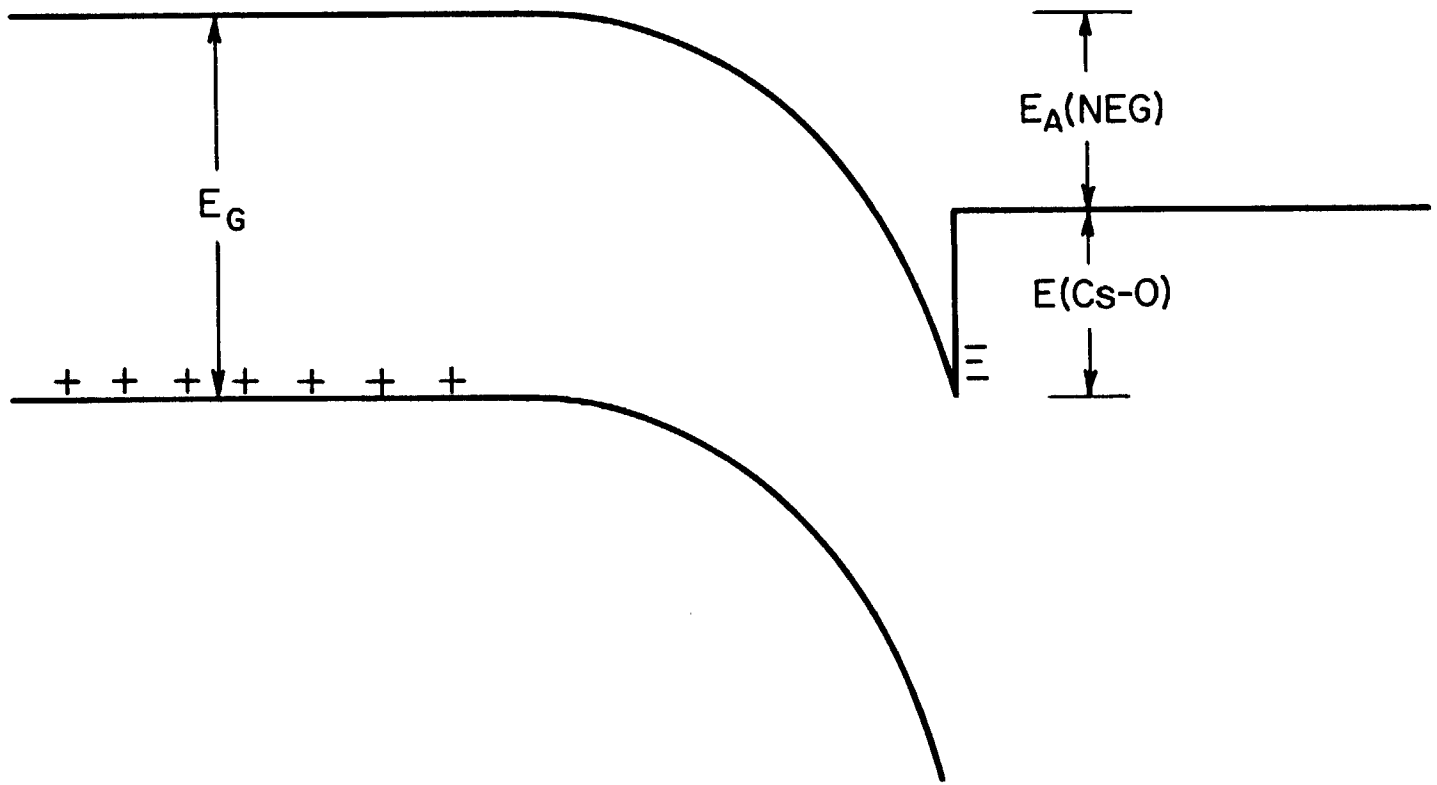

FIG. 3. BENT-BAND MODEL (NEGATIVE ELECTRON AFFINITY)

electron in the conduction band of GaP is 10^{-9} or 10^{-10} sec and the escape depth may be a micron or more for these new emitters.

As a result, the secondary emission ratio, which has a maximum on the order of 10 or so for conventional CuBe or AgMg dynode materials, has been measured as high as 150 for GaP:Cs and, theoretically, may go as high as 500 or 600. It is expected that the new dynode materials will replace the old in all multipliers in the near future.

The argument, which has been stated in words, can be put on a much more quantitative basis. The theory assumes that the secondary emission ratio δ can be expressed as

$$d\delta = n(x,V)f(x)B\ dx$$

where $n(x,V)$ is the number of electrons excited per unit path by the primary electron of energy corresponding to potential V at the distance x from the surface. The probability that an electron produced at x reaches the surface is given by $f(x)$ and that it is emitted from the surface by B.

It is now necessary to evaluate the various functions. Each excitation deducts a certain energy from the incident electron, and we can, without serious loss of accuracy, conclude that the linear density of excitation will be proportional to the energy loss per unit length of primary particle path. If the energy loss density is assumed constant over the range R of the primary electron, we have

$$n(V,x) = \frac{1}{\epsilon}\frac{dV}{dx} = \frac{V}{\epsilon R}$$

where ϵ is the energy used for each excitation. The range R varies somewhat faster than linearly, and probably the exact form of the function depends upon the material involved.[8] It has been variously reported to be from $R \sim V^{1.33}$ to $R \sim V^{2}$. The former seems to give a good fit for GaP secondary emission while the latter has been used very successfully to account for the behavior of silicon solid state nuclear radiation detectors for β-rays.

The diffusion of the excited electron to the surface is a complicated process. While the mechanisms are very different for "hot" electrons in conventional secondary emitters and for the thermally diffusing electrons of the new bent-band emitters, they both are statistical processes, and the loss of particles varies exponentially with path length (i.e., distance x between point of excitation and point of emission. Thus,

$$f(x) = e^{-x/L}$$

where L is the mean path between the excitation and the point where the electron loses so much energy that it cannot escape. In the conventional emitter, it is where the energy falls below the electron affinity, and, for the newer secondary emitters, it is where the electron drops out of the conduction band.

Combining these relationships, we have

$$\delta = \int_0^R \frac{B_s V}{eR} e^{-x/L_s} \, dx$$

$$= \frac{B_s L_s}{Re} V \, (1 - e^{-R/L_s}) \qquad (1)$$

and $$R = AV^{1.35}$$

The form of the function describing secondary emission is illustrated in Fig. 4.

This general secondary emission function has been very successful in tying together the experimental observations from a wide variety of emitters including the bent-band secondary emitting materials. In this equation B_s is a measure of the emissive properties of the surface while L_s describes the transport properties of the bulk material. It is possible to evaluate L_s and B_s independently by using a wide range of voltages. (See Appendix). An attempt has been made to determine whether fatigue was primarily due to surface damage or whether it also included a bulk effect by using this technique. Secondary emission ratios as a function of primary voltage will be shown in a later section for fresh and fatigued GaP emitters.

Photoemission, particularly of the bent-band emitters, can be expressed in terms of the same parameters. A comparison of photoemission and secondary emission before and after an emitter is fatigued should also differentiate between bulk and surface effects.

The photoemissive yield Y of a material can be expressed in terms which are closely related to the B and L of Eq. (1). An analysis of the photoemissive behavior before and after fatiguing is particularly valuable in the case of the bent-band emitters because the mean free paths are great enough so that one can assume bulk optical absorption properties obtain.

In photoemission, the transport and escape mechanisms are essentially the same as for secondary emission. However, the excitation will be different. We will assume that absorption occurs because photons are removed from the incident light, giving up their energy in producing

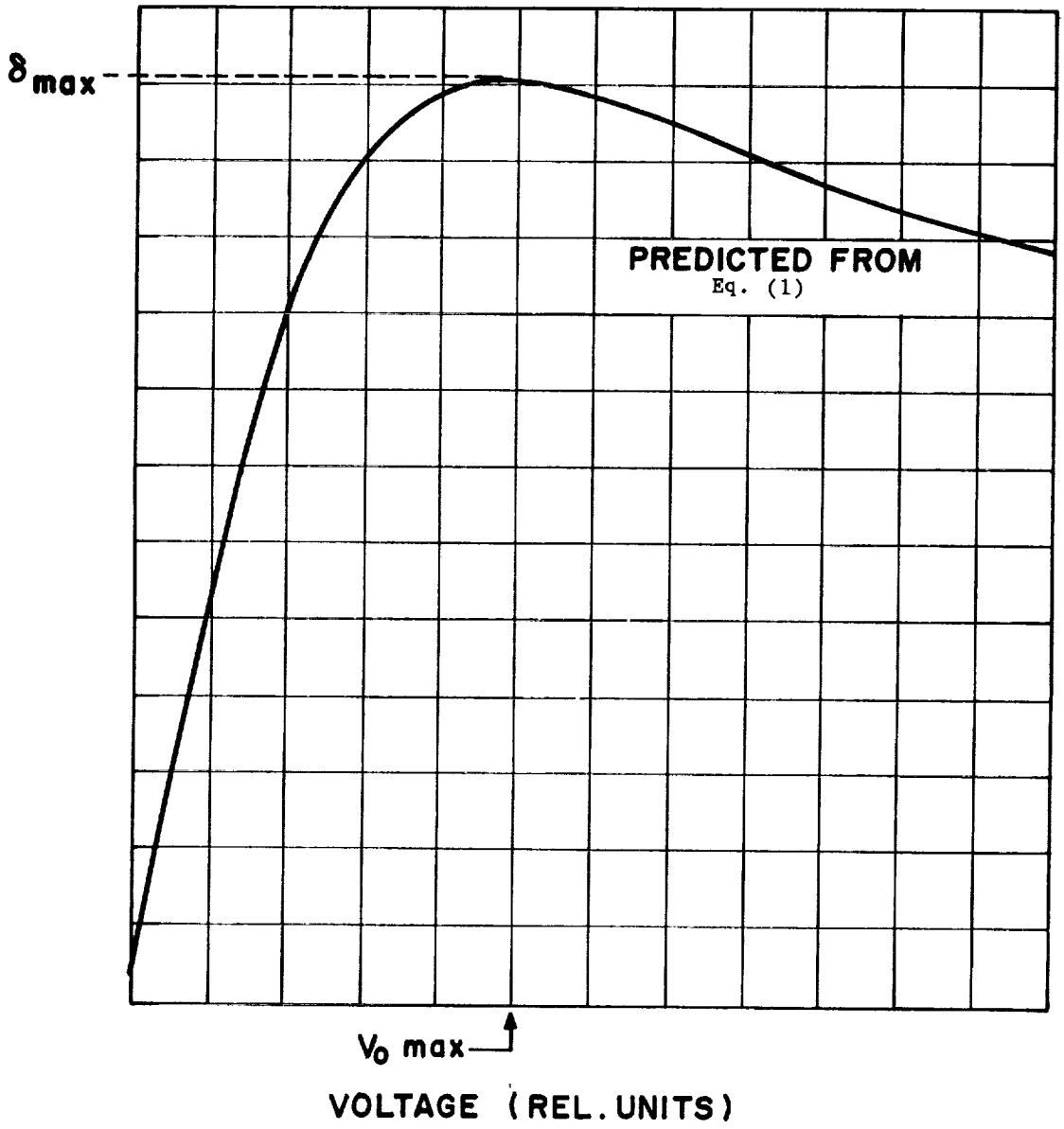

FIG. 4. GENERAL SECONDARY EMISSION CURVE

excitation. If the sample is illuminated from the emitting side and has an optical absorption coefficient α, photoelectrons will be excited at point x in the crystal at a rate

$$dn = I(1-R)e^{-\alpha x}\alpha dx$$

where I is the incident illumination (photons/sec) and R the reflectivity.

The expression for emission therefore will be

$$Y = (1-R)B_p\int_o^\infty \alpha dx e^{-\alpha x}e^{-x/L_p}$$

This integrates to

$$[Y/1-R]^{-1} = \frac{1}{B_p} + \frac{1}{B_pL_p}(\alpha^{-1}) \qquad (2)$$

Therefore, if one plots reciprocal yield against absorption coefficient (over a limited wavelength range), one obtains $1/B_p$ as an intercept and $1/B_pL_p$ as the slope of the resulting line. Hence B_p and L_p can be evaluated. (See Appendix) This is a very powerful tool for the study of the cause of fatigue in secondary emitters when the results are compared with the variation of gain δ with primary electron energy V_o before and after fatiguing.

As will be discussed in greater detail in the Appendix, a start was made on the application of this analysis to the problem, but time did not permit the completion of the study.

It was not possible in the course of this program to work out a procedure for overcoming fatigue in photomultipliers either of the conventional type or those using GaP dynodes. Therefore two circuit methods of reducing the effects of fatigue, namely, photon counting and feedback stabilization, will be discussed.

As was explained above, much of the work of this phase was centered around the study of fatigue in multipliers using GaP dynodes. One of the reasons that they will displace conventional multipliers is because of their excellent pulse counting capabilities. This means that they are very good for photon counting and photon counting is the most accurate way of carrying out radiometry at low light levels. By combining a photomultiplier with a calibrated controllable attenuator, pulse counting can be used over any range of light level desired. For reasons that are discussed later in Section V, the new high-gain dynodes make it possible to use multipliers in the photon counting mode in such a way that there can be a considerable change in gain due to fatigue without introducing appreciable error. To show that this is to be expected, the quantitative

aspect (in the statistics) of pulse height distribution from a multiplier will be considered in Section V.

It is possible to use a very constant (amplitude) pulsed light source as a means of stablizing the gain of a multiplier. Here, the calibrating signal time shares with the signal to be measured and serves to control the multiplier voltage in such a way as to hold the gain constant. Details of this type of stabilization are given in Section VI.

III. FATIGUE IN PHOTOMULTIPLIERS WITH CuBe AND AgMg DYNODES

The decrease of gain during operation or fatigue for four fairly typical conventional multipliers is shown in Fig. 5. The data are plotted as relative gain (not, however, normalized) vs log Q where Q is $\int_0^t i_A dt$. In general, during operation the fatiguing output was kept constant throughout the run. During this time, the monitoring 2000-cycle pulses from the cathode were held constant.

It will be noted that over fairly large portions of the runs on each tube the decrease in gain was nearly logarithmic in time (charge). However, almost all the tubes showed some irregularities in their behavior.

The tubes included both those with AgMg dynodes (7264) and CuBe dynodes (7850) and the developmental tube (C70101AX). There is little difference seen in the behavior of the two types of dynode, and the fatigue rates of the CuBe tubes bracket that of the MgAg multipliers.

Fatigue is to an extent reversible. If, after the tube has been operated for a time and fatigued, it is allowed to stand with no current flowing through it, it will recover some of the lost gain. In many instances, the recovery is nearly complete.

Although complete experimental confirmation is still not available, it appears that the recovery process continues whether the tube is operating or not and that the specific recovery rate increases with increasing damage. If this is true, then any tube, if operated for a long enough period at any one current, will come to an equilibrium such that the fatigue rate and recovery rate are equal.

There is also some evidence that, if a tube is cycled through a number of decay and recovery periods, it will, at least for low light levels, reach a condition where the tube gain is much more stable than it was initially.

During the first phase of the research, there seemed to be some evidence indicating that, if a low pressure of argon was left in a tube, the decay rate was greatly decreased. A gas-handling manifold with ion pumps and bakable vacuum valves was built to test this point. It was found that the observation could not be repeated, and the tubes tested, though they showed certain anomalies, in general did not show gain stabilization.

In order to confirm that the fatigue was not solely due to the migration of Cs onto and from the dynode surfaces, tests were made on a tube

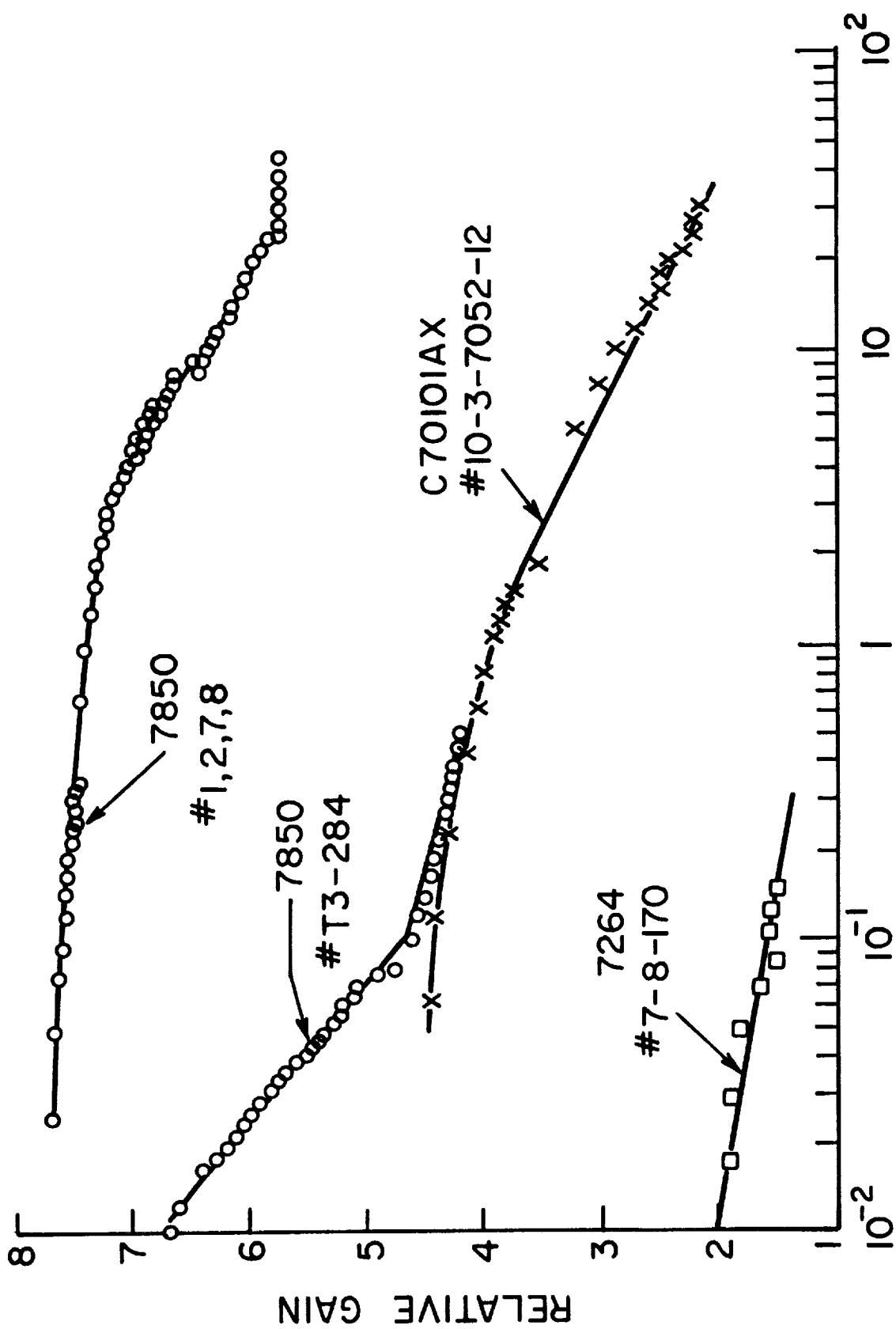

FIG. 5. FATIGUE IN FOUR CONVENTIONAL MULTIPLIERS

which had a Na_2KSb photocathode and uncesiated CuBe dynodes. The fatigue rate of this tube was very nearly the same as that of tubes containing cesium. It might also be pointed out that earlier experiments on non-cesiated high-gain MgO surfaces showed strong deterioration under electron bombardment, as do NaCl and KCl secondary emitters.

Some tests were made to determine whether at very low voltage the fatigue would be less than at higher voltage. Over the range covered, the indications were that the fatigue was relatively independent of voltage.

The only conclusions, for multipliers with conventional dynodes, that can be drawn so far are the following:

(1) The cause and nature of fatigue are not known.

(2) Insulators supporting the dynodes should be arranged so that they do not become charged by the multiplier electron space current and alter electron optical paths.

(3) The activation should involve the minimum of cesium required for good gain, and the tube should be well baked and aged inasmuch as loosely bound cesium can introduce gain instabilities.

(4) Where the illumination is fairly constant, the tube can be pre-fatigued so that the fatigue rates and recovery rates are nearly equal. Alternate cycling of operating and recovery periods sometimes helps to stabilize the gain.

(5) Additional gain stabilization can be obtained through feedback circuits controlling the over-all voltage in electron-optical focus and actuated by a calibrating light which "time shares" for a small fraction of the operating time of the multiplier with the light being measured. See Section VI.

IV. FATIGUE IN MULTIPLIERS WITH HIGH-GAIN DYNODES

Two approaches were used in the investigation of fatigue in the new high-gain GaP dynodes. The first was the study of the performance of a photomultiplier with six GaP dynodes. The second was with a measuring tube having an electron gun as the source of primary electrons and a target in the form of a GaP dynode. In addition, some fatigue and life performance data were obtained from the multiplier development and production units.

The six-stage tube used in the fatigue tests had a photocathode-first dynode electron optical system identical with that of the 7850. The pin arrangement was such that the tube could be plugged into a socket wired for a conventional 7850 and the voltages would be such that there would be equal voltage steps from dynode 1 to dynode 6 and the voltage between the cathode and first dynode would be twice the interstage voltage. This was so that the gain of the first dynode would be as large as possible without over-voltaging the multiplier. This was done because in analyzing the pulse performance of the device it can be shown that, next to photocathode sensitivity, the gain of the first dynode is the most important factor in determining pulse height resolution. Under these conditions of operation and where the number of photoelectrons per flash N_e is small (3 to 6 or 8), the spectrum breaks up into a series of peaks representing the frequency of single electrons, electron pairs, triplets, and so on. More will be said about this in the discussion of photon counting for radiometry.

Since in practice this type of voltage distribution with a large cathode to D_1 voltage is used for these new multipliers, it was thought advisable to use it in fatigue tests. This tube could be used with the measuring and recording equipment discussed earlier.

The measured initial dynode gains of the six-stage tube were disappointingly low. They measured as follows:

Dynode No.	Gain δ_n at 450 v
1	6.9
2	13
3	11.5
4	6.85
5	3.5
6	3.5

For the relatively high current tests desired, dynode 6 is the dynode that should be examined. However, its initial gain is so low that it does not represent a typical GaP surface.

The tube was operated monitoring the anode and dynode 6 current; thus,

$$\delta_6 = \frac{i_a}{i_a - i_6}$$

The fatigue test was continued for 1000 hours with three recovery periods. The gain behavior is shown in Fig. 6.

The dynode dropped from 3 to 2.85 in the first 100-hour run. In the next 100 hours, with no light, it recovered all its lost gain (i.e., $\delta_6 \longrightarrow 3.1$). This was repeated two more times with nearly complete recovery. This can be taken to mean that the GaP shows the same characteristic fatigue and recovery that appears to be present in all dynode materials. As the tube was cycled, the change in gain may have decreased to a certain extent. This is in line with the qualitative observation that aging may decrease (but not eliminate) fatigue effects.

Much more controlled experiments could be done with the demountable gun tube with a single GaP dynode sample. The measuring tube is shown diagrammed in Fig. 7. The gun is a standard high-voltage unit but employed a thoriated tantalum cathode to reduce sample contamination. Flanges with gold O-rings were provided at both ends to permit replacing the secondary emitter sample and the gun cathode. An internal cesium channel was used as the source of cesium to activate the sample, and oxygen was supplied from an electrically-heated silver side tube. The tube was processed on a mercury diffusion pump system, then sealed off and the vacuum maintained with a 1 liter/sec Vac-Ion pump.

Four gallium phosphide emitters were tested with this unit. Each sample required many hours of activation, processing, and measuring and each many hundreds of hours fatiguing time. The four test samples will be designated A, B, C, and D, more or less in chronological order.

In the investigation of these secondary emitting surfaces, an attempt was made in each case to determine

(1) the fatigue characteristics,

(2) variation of secondary emission ratio δ with primary electron voltage before and after the life test run,

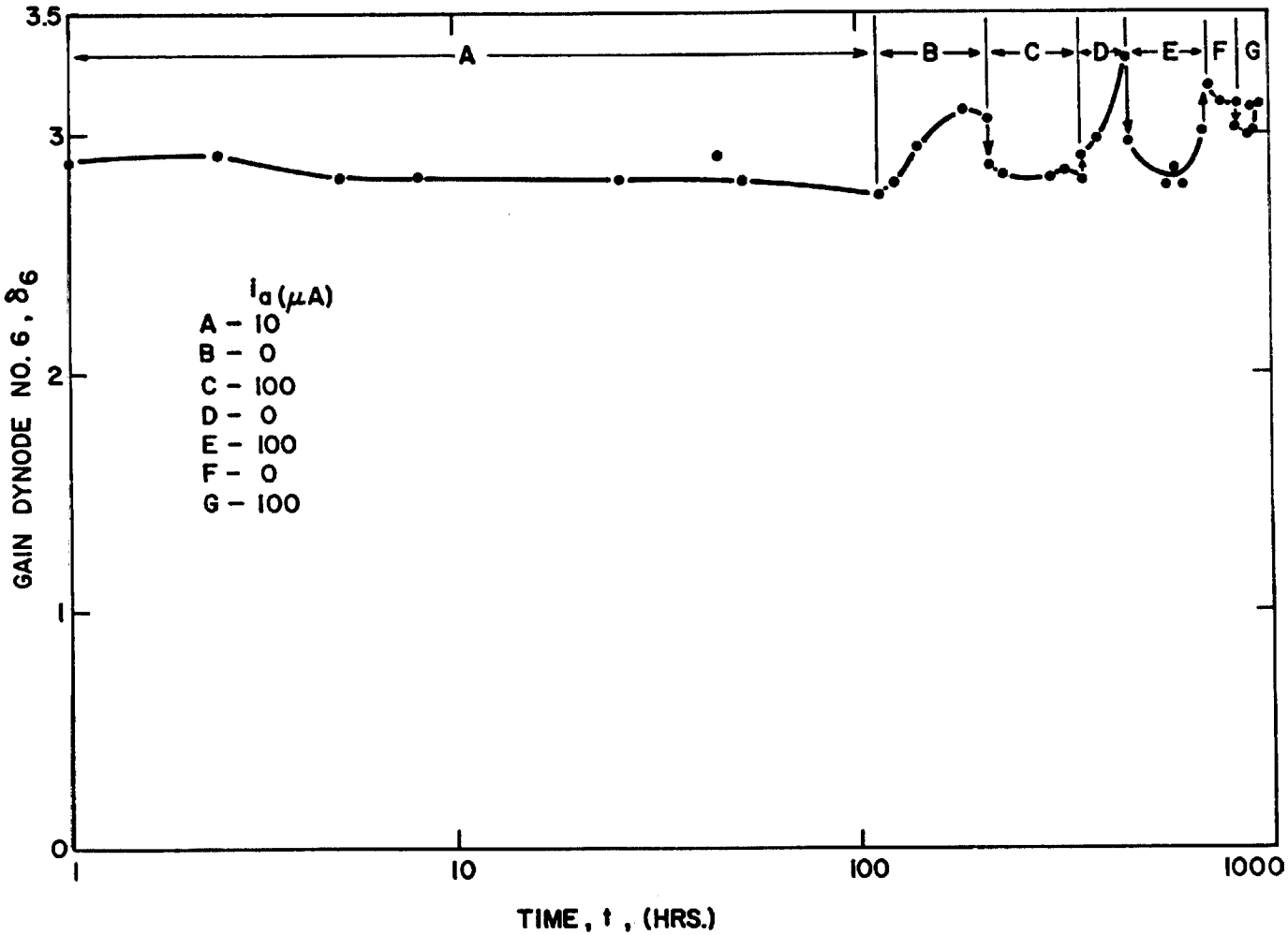

FIG. 6. FATIGUE CHARACTERISTICS OF DYNODE 6 OF A GaP DYNODE PHOTOMULTIPLIER

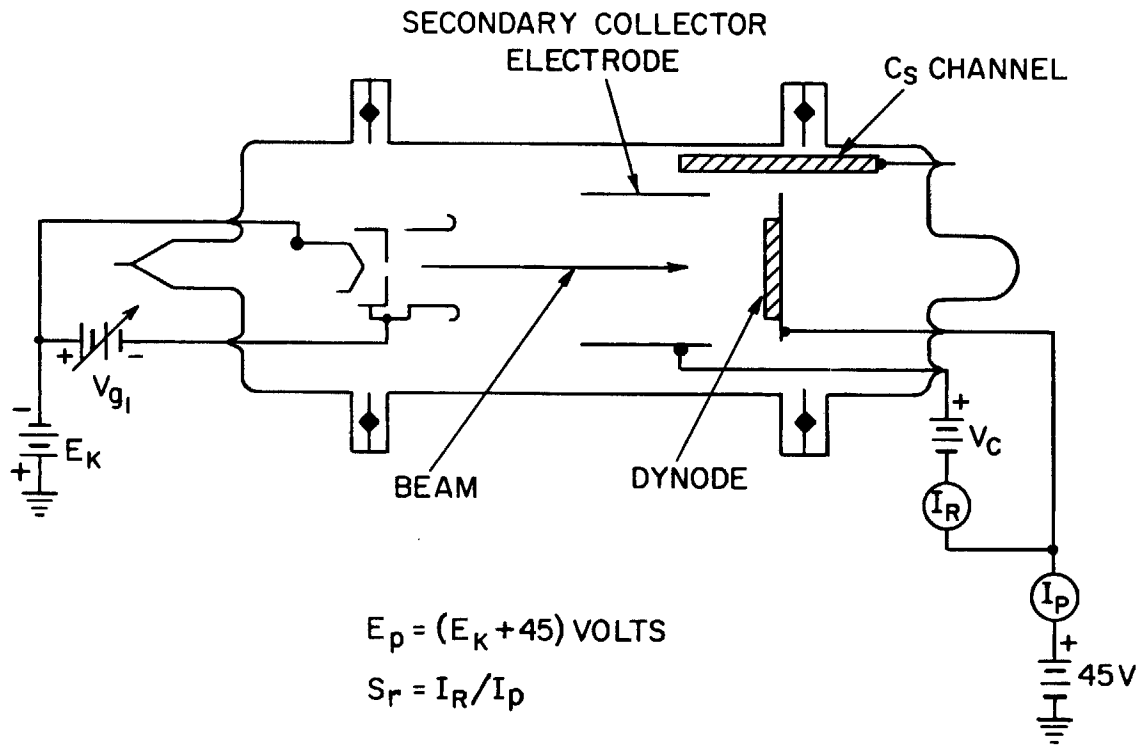

FIG. 7. SCHEMATIC DIAGRAM OF DEMOUNTABLE SINGLE DYNODE TEST TUBE WITH ELECTRON GUN

(3) photoelectric yield as a function of wavelength before and after fatiguing, and

(4) comparison of B and L, the surface escape probability and the escape depth, respectively, for secondary emission and photoemission as calculated from results of (2) and (3).

Only part of this program could be accomplished because of the difficulties of the experiments and the lack of time.

Before discussing the general behavior of the material as it fatigues, the behavior of the four individual GaP samples A, B, C, and D, together with a fifth GaP specimen E which was not fatigue-tested, will be presented in the following subsections.

Sample A. This sample was activated in the normal way and exhibited a secondary emission ratio δ vs voltage varied to fit $B_s = .350$ and $L_s = 2660$ Å in Eq. (1). The two constants E and A have values of 8.7 and 1710, respectively. (See Appendix) The photoresponse was 6.0 μA/lm and δ at 1000 v was 30. Operating at 500 volts and 2 nA (see Fig. 8, Curve a), δ went from 20 to 5.6 in 350 hours. At the end point, the photoemission was very low.

The dynode was reactivated with a cesium and thermal treatment. At this point $\delta_{1000} = 12$ and photoemission = 3.0 μA/lm. The quantum efficiency as a function of wavelength was measured so that B and L could be calculated as described in Section III. The values were found to be

$$B_p = 0.084$$
$$L_p = 2100 \text{ Å}$$

The sample was fatigued for an additional 200 hours at 1000 volts and 3 μA. In this period δ_{1000} went from 12 to 6.6. The spectral quantum efficiency was again taken and B and L determined as

$$B_p = .032$$
$$L_p = 1800 \text{ Å}$$

The fatiguing process was continued under the same conditions for 200 hours more. During this time δ_{1000} went from 6.6 to 4.7. The photoresponse was so low that B and L could not be accurately determined. This experiment was terminated. The fatigue of the reactivated surface is shown as Curve b in Fig. 8.

Sample B. This sample was activated by the same schedule used for Sample A. Its gain δ at 500 v was 24.7 and its photoelectric response was

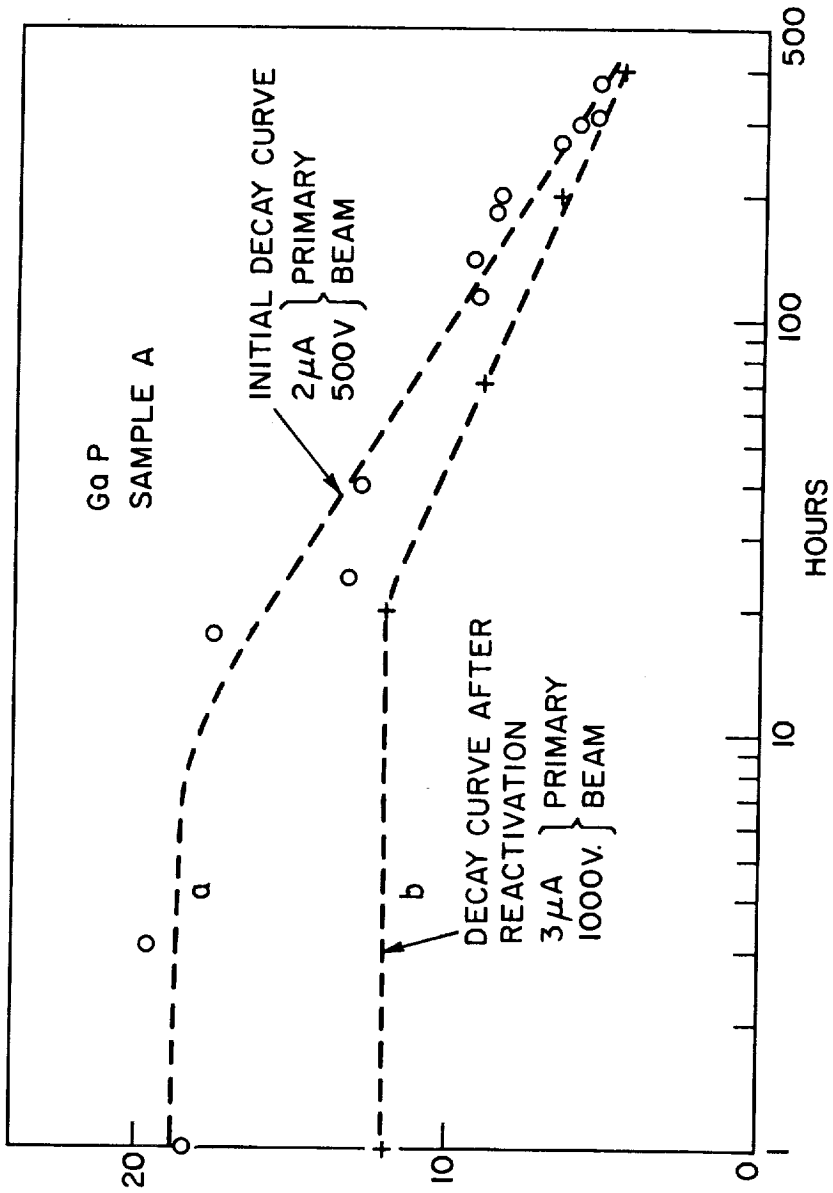

FIG. 8. FATIGUE CURVES FOR SAMPLE A

4.5 μA/lm whole light and 1.7 μA/lm filtered with the blue Corning No. 5-58 filter (1/2 stock thickness). The photoelectric spectral response measurements gave

$$B_p = .158$$
$$L_p = 2200 \text{ Å}$$

The gain δ as a function of voltage before fatiguing is shown in Fig. 9 as Curve a. This curve is for an escape depth of $L_s = 2200$ Å and an escape probability of $B_s = 0.605$. The measured secondary emission points are shown on the figure. Upon fatiguing with a .4 μA beam at 500 volts, the gain δ dropped very rapidly. At the end of about 30 hours, it had gone from about 24 to 8. The gain after fatigue as a function of voltage is shown in Fig. 9, Curve b. At this point $L_s = 1520$ and $B_s = 0.160$ as determined from the secondary emission curve. B and L were again determined from the photoelectric response and were found to be

$$B_p = .0112$$
$$L_p = 3650 \text{ Å}$$

The sample was reactivated and measured as Sample B_2. The initial gain of the reactivated specimen at 500 volts was about 10 and 18 at 2000 volts which is the peak of its secondary emission ratio. From the secondary emission vs voltage curve, B_s and L_s were found to be 0.20 and 1820 Å, respectively. The corresponding values from photoemission are $B_p = 0.56$ and $L = 1170$ Å. The sample was fatigued for a period of 70 hours with the gain going from 10 to 5.2. During this time, the collector voltage was 7.5 volts. The operation was continued with the same primary voltage and current but the collector voltage was increased to 300 volts. There was no discontinuity in the rate of decay. The run was continued another 100 hours with the gain δ dropping to 3.9. The fatigue curve for this test is shown as Curve B_2 in Fig. 10. The absence of any change in the rate of decay with increase of collector voltage means that positive ions do not play an essential role in this fatigue problem. The gain δ vs voltage is shown in Fig. 11 both before and after the fatigue test. At the end of the test, the two coefficients of the secondary emission equation were $B_s = 0.145$ and $L_s = 460$ Å. The photoelectric response was too small to obtain the corresponding B_p and L_p values for photoemission.

Sample C. This sample was done in a sealed-off gun tube. Its photosensitivity to whole light was 9 μA/lm and 3.5 μA/lm with the blue filter. It had a secondary emission ratio δ of 21 at 500 volts before fatiguing. Fig. 12 is a curve of the gain δ vs log time. The photoemission spectral response yielded

$$B_p = 0.52$$
$$L_p = 1400 \text{ Å}$$

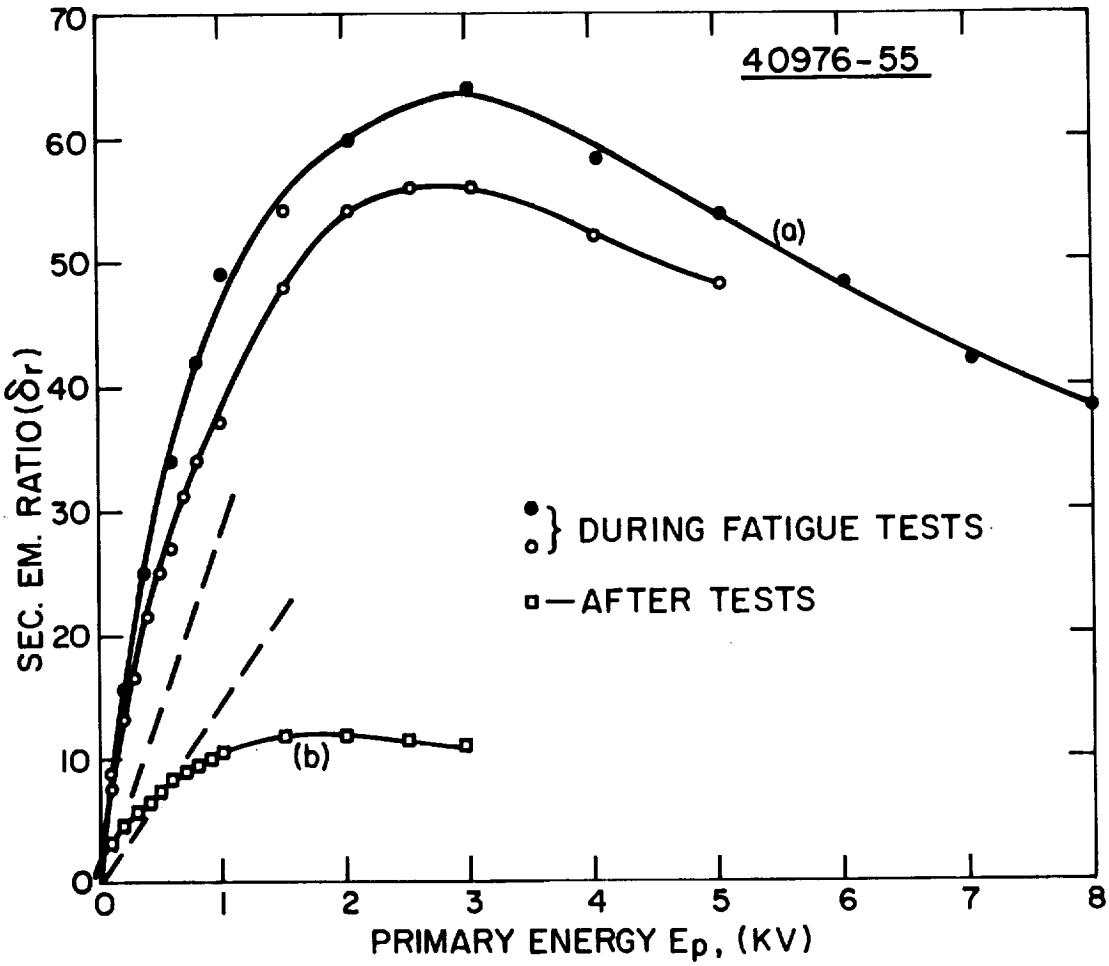

FIG. 9. GAIN VS VOLTAGE SAMPLE B (1st ACTIVATION)(START OF RUN (a)) (AFTER 30 HRS. (b))

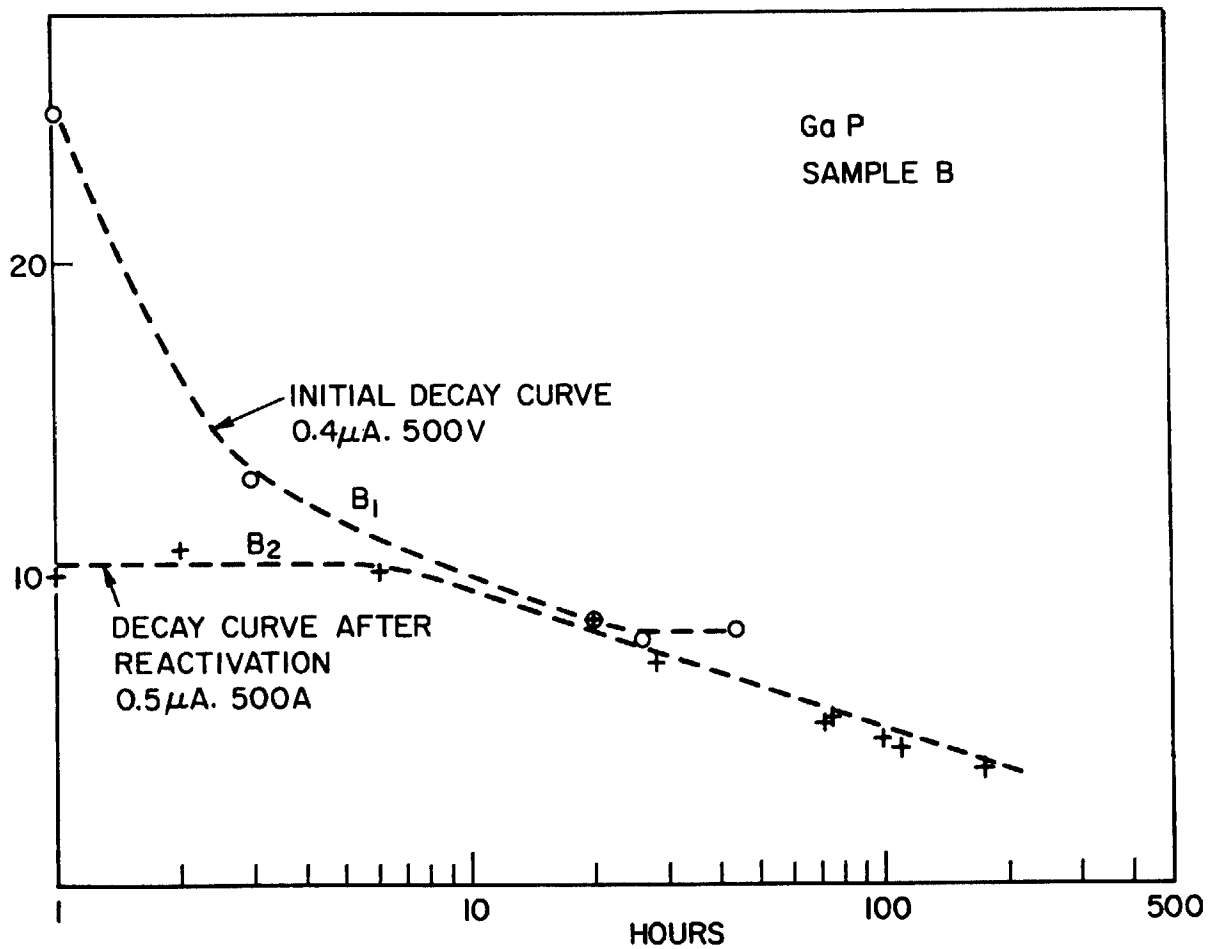

FIG. 10. FATIGUE CURVE SAMPLE B (B_1 FIRST ACTIVATION, B_2 REACTIVATION)

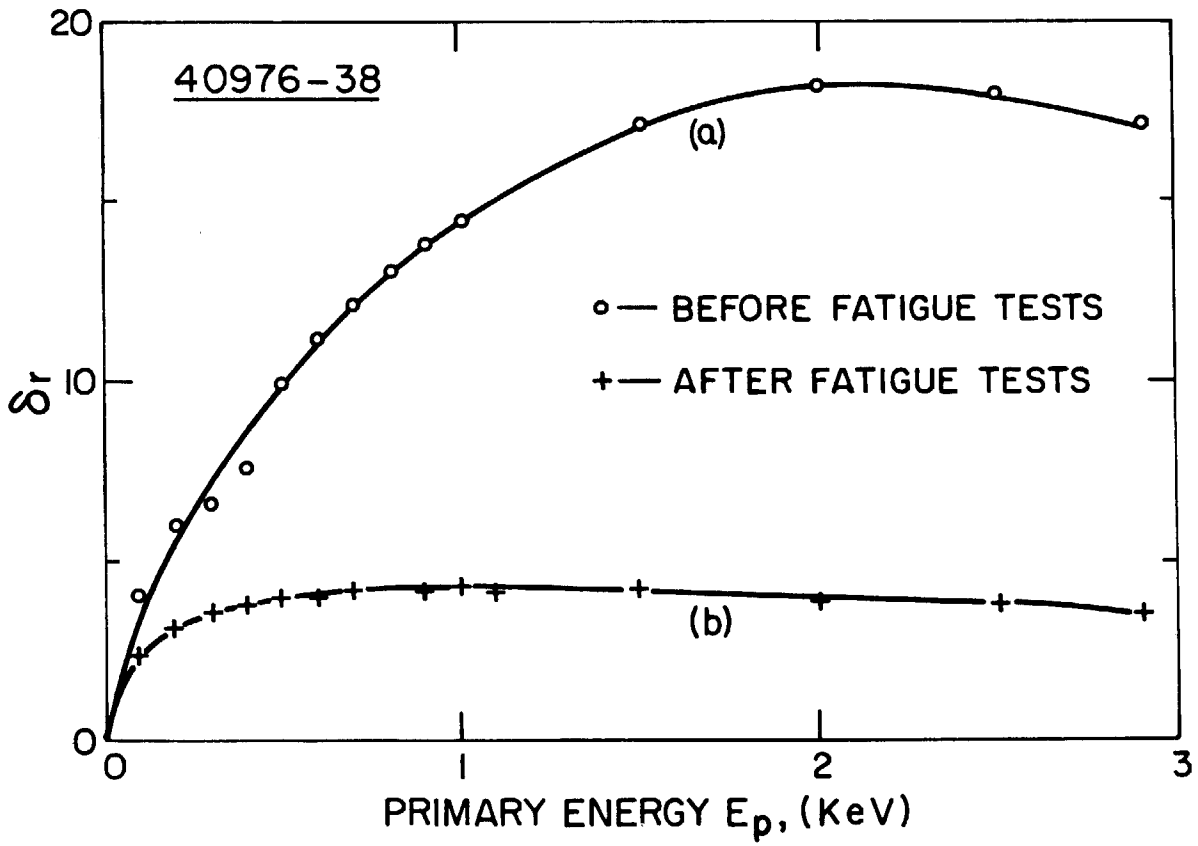

FIG. 11. GAIN VS VOLTAGE SAMPLE B_2 (2nd ACTIVATION)(START OF FATIGUE A AND AFTER 100 HRS. B)

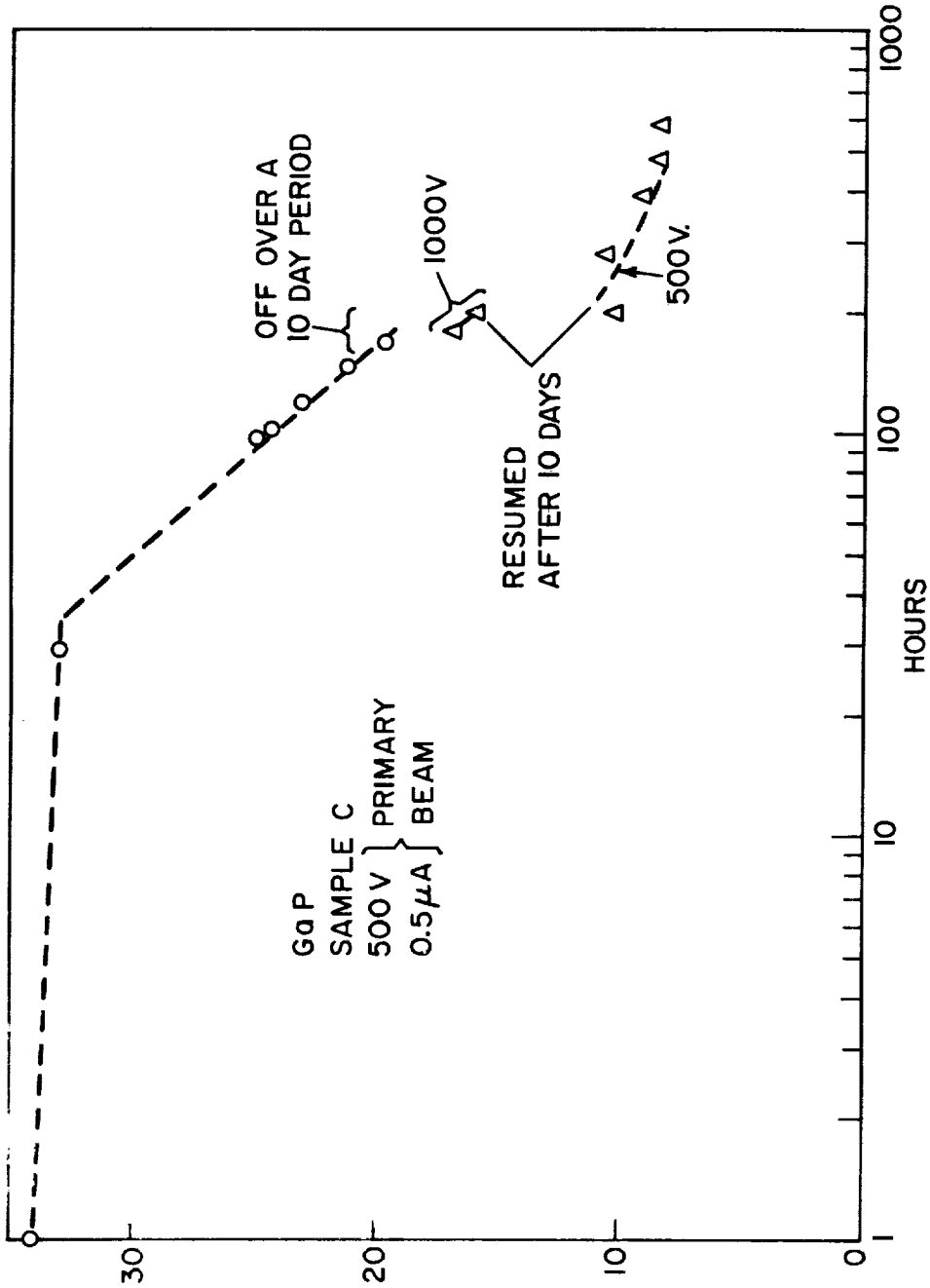

FIG. 12. FATIGUE CURVE SAMPLE C

while from the secondary emission curve

$$B_s = 0.375$$
$$L_s = 2740 \text{ Å}$$

The sample was operated for 80 hours at 500 volts and 0.5 μA, during which time it showed little or no decrease in δ. The primary voltage was raised to 1000 volts. Over the next 150 hours the gain δ dropped from 34 to about 20. The tube was left, with cathode heater on but no primary voltage applied, for a period of 10 days. There was little change in δ. Fatiguing was resumed at 1000 volts with a 0.5 μA beam, and then at 500 volts. The gain decreased only very slightly in an additional 350 hours. At this point the tube failed so that gain δ vs V and photoemissive response measurements could not be made.

Sample D. Sample D was also in a sealed-off tube and activated by the same standard process used for the other samples. Photoemissive spectral measurements gave the following values for the escape depth and escape probability:

$$B_p = .133$$
$$L_p = 1213 \text{ Å}$$

The secondary emission ratio as a function of time is given in Fig. 13. At 500 volts the secondary emission ratio was 13.6. The maximum δ was about 40 and occurred between 3000 and 3500 volts. The values for the emission probability and escape depth for secondary emission were

$$B_s = 0.24$$
$$L_s = 4000 \text{ Å}$$

The tube was fatigued for a period of 3 hours with a beam current of 0.3 μA at 500 volts. During this period the gain dropped from ~14 to 10. The cathode heater became open-circuited at the end of this period, and the tests had to be discontinued.

Sample E. Sample E was not used in fatigue tests but is discussed as part of the attempt to correlate photoemissive behavior with its performance as a secondary emitter. Fig. A-2 shows the secondary emission ratio δ as a function of voltage. From these data the values obtained for the emission probability and escape depth are

$$B_s = 0.495$$
$$L_s = 2100 \text{ Å}$$

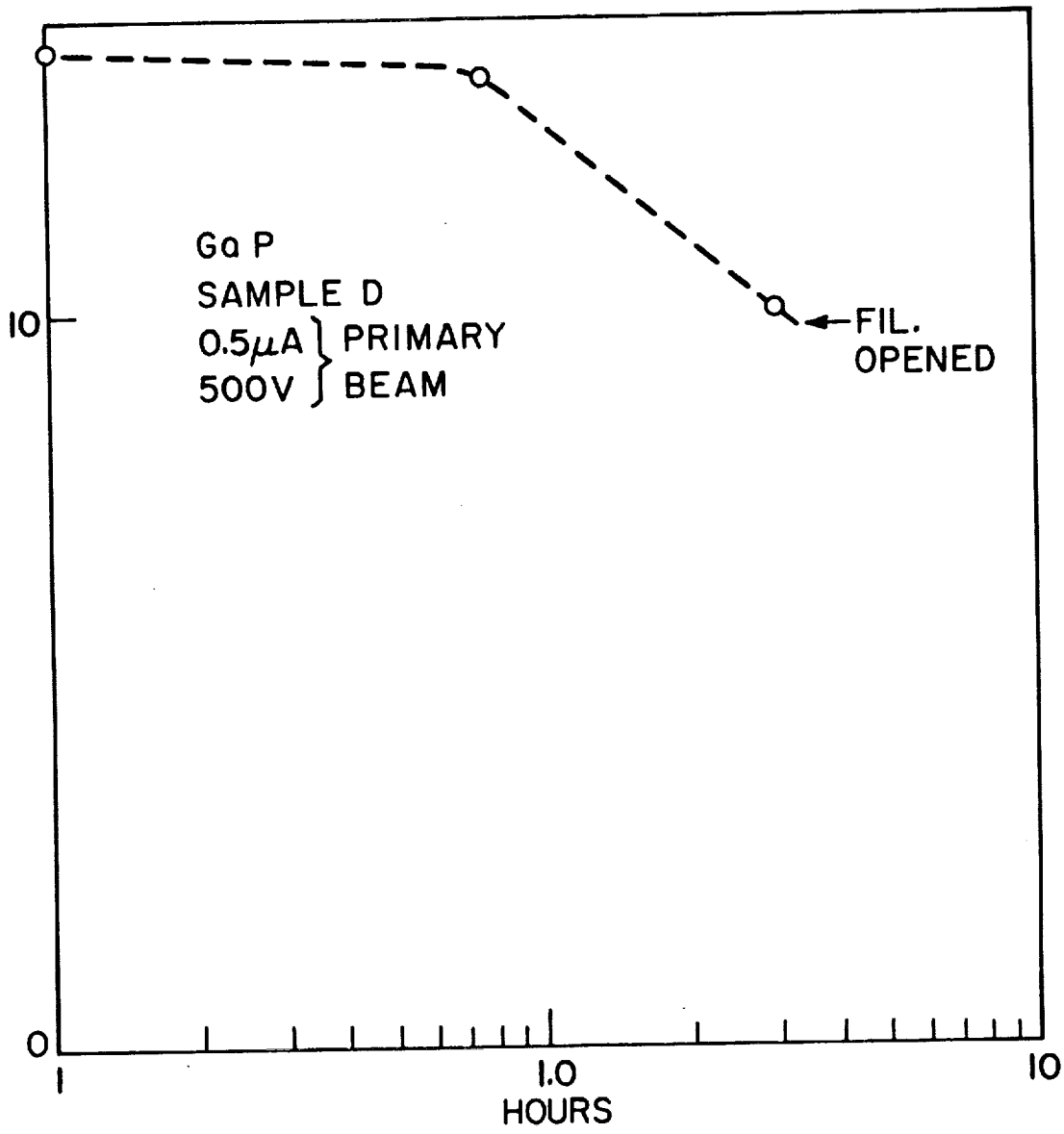

FIG. 13 FATIGUE CURVE SAMPLE D

Photoemissive measurements yield values of

$$B_p = .39$$
$$L_p = 4200 \text{ Å}$$

Discussion. From the data obtained from the five samples, it has not been possible to form anything like a coherent picture of the mechanism involved in the fatigue process in GaP secondary emitters. In Fig. 14 fatigue data, with gain normalized to unity at the start of each experiment is shown plotted as a function of the logarithm of the charge incident on the specimen during the course of the test. In each case, the area over which the beam was incident was a spot approximately one-half centimeter in diameter. The current density over the bombarded area was not uniform but probably did not change significantly from sample to sample.

It is probably fortuitous that the behavior of all of the samples is so nearly alike and has essentially the same rate of decay with the logarithm of time after an initial period of fairly constant gain.

These curves show that, after a surface has been fatigued to its 50% point, the rate of fatigue (as a linear function) is very small and, for many purposes, a multiplier with "aged" dynodes will be sufficiently stable.

In the case of high-gain GaP dynodes, recovery after fatigue appears to be much less pronounced than with normal low-gain emitters or with low-gain GaP.

Where possible, measurements were made of secondary emission ratios as a function of voltage at the start and end of fatigue runs. Unfortunately, in several instances the fatigue run was terminated by tube failure and the gain curve could not be measured. From the data obtained, it was found that the curve giving the gain as a function of voltage was changed in shape as well as height. In general, the shape change resulted in the maximum yield occurring at a lower voltage than with an unfatigued dynode. This is shown as a decrease in escape depth L_s in the general secondary emission formula. For example, with Sample B in its first activation $L_p = 2200$ Å while after about 30 hours L_p had dropped to 1500 Å, the gain had gone from 25 to 8, and the peak gain of 64 at 2500 volts had dropped to 12 at 1800 volts. Similarly, upon reactivation $L_s = 1800$ Å with the gain being 18 at 2100 volts which, after about 200 hours, dropped to $L_s = 460$ Å with the peak gain becoming 4.4 at 1000 volts.

Correlation between B_p and B_s and L_p and L_s of Eq. (1) and Eq. (2) comparing photoelectric data with secondary emission data is not good.

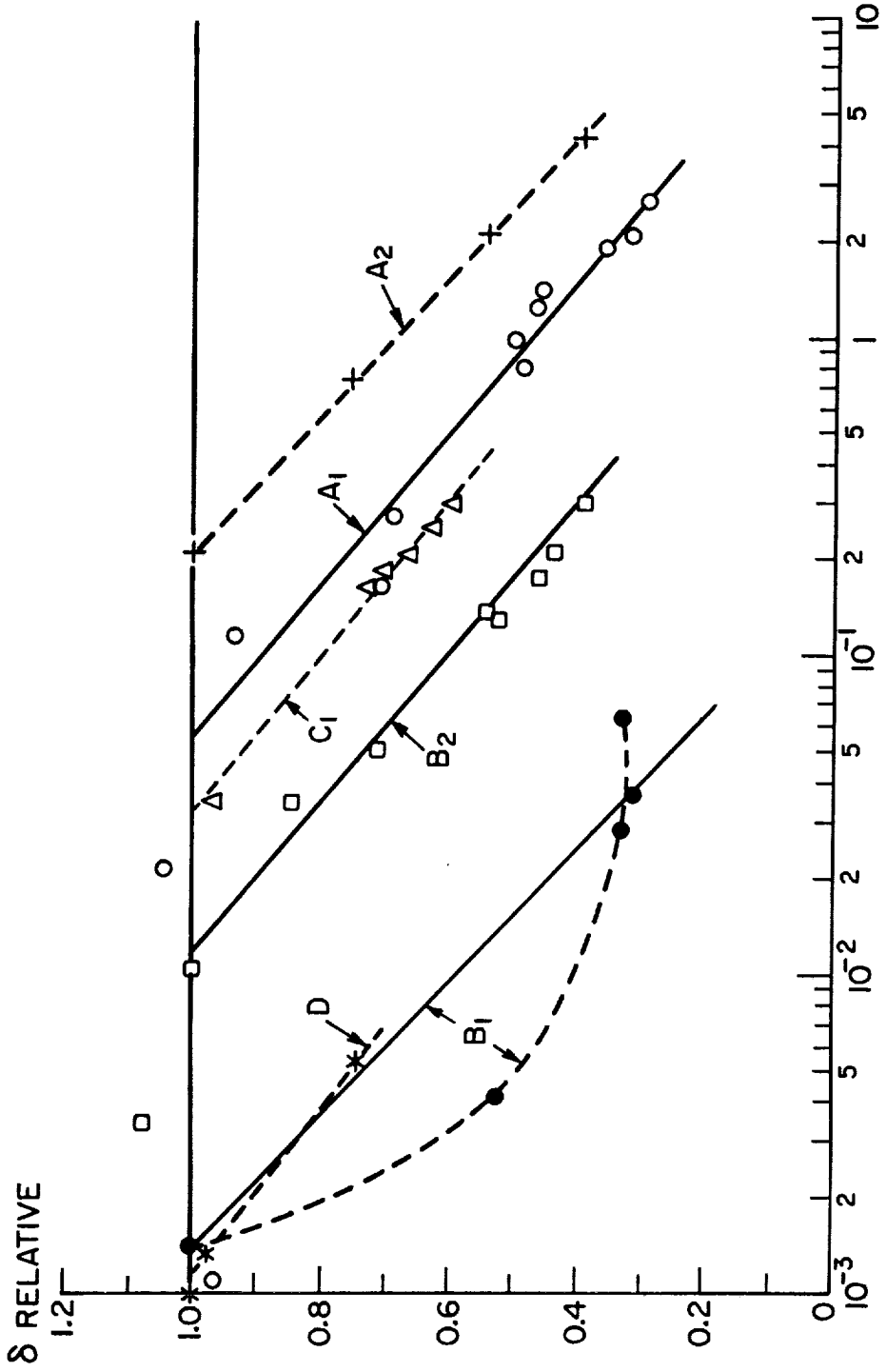

FIG. 14. NORMALIZED FATIGUE CURVES FOR SAMPLES A, B, C, AND D

However, measurement of changes in any one dynode before and after fatiguing point to the same thing, namely, that both the escape probability and the escape depth are decreased by fatigue. For example, two measurements made on Sample A 100 operating hours apart give

$$\left.\begin{aligned} \delta_{start} &= 12 \\ B_p &= .084 \\ L_p &= 2100\ \text{Å} \end{aligned}\right\} \text{ after } 100 \text{ hrs } \left\{\begin{aligned} \delta_{end} &= 6.55 \\ B_p &= .032 \\ L_p &= 1800\ \text{Å} \end{aligned}\right.$$

Again, with Sample B, in its first run the first photoemission measurement can be compared with that 30 hours later:

$$\left.\begin{aligned} \delta_{start} &= 24.6 \\ B_p &= .095 \\ L_p &= 4900\ \text{Å} \end{aligned}\right\} \text{ after } 30 \text{ hrs } \left\{\begin{aligned} \delta_{end} &= 8.4 \\ B_p &= .0112 \\ L_p &= 3650\ \text{Å} \end{aligned}\right.$$

The interesting conclusion that seems to be indicated by both the secondary emission and photoelectric data is that the change is not merely a surface change. The escape probability is in every case reduced. However, the escape depth is also decreased. Since the change in escape depth, which, for one thing, decreases the voltage at which maximum secondary emission occurs, seems to involve distances in the material beyond the range of the electrons causing the fatiguing, it is probable that interpreting L literally as a drift or diffusion distance is an oversimplification of the model. It is probable that the quantity L may also include the effect of such things as a potential barrier from which energetic electrons moving away from the surface may be reflected and escape. Much more research on the general problem of fatigue will be required before a good model can be deduced. So far, no good physical model has been found nor has a way of eliminating fatigue been found.

Because of the universality of the phenomenon of fatigue - both with respect to materials and shape of the fatigue curve as a function of time - the finding of a surface material or a surface treatment which will overcome fatigue is very unlikely. There is evidence to indicate that fatigue can be reduced by aging a surface and that it occurs at a slower rate for low primary voltage; neither of these can be considered as a way of overcoming fatigue.

V. PHOTON COUNTING[10]

The most sensitive and accurate way of making absolute photometric measurements with a photomultiplier is by photon counting. By photon counting is meant the processing of the pulses at the output of the phototube due to the individual photoelectrons from the photocathode in such a way that each pulse contributes the same amount to the output signal from a display presentation device. The display may give a numeric count of the pulses or it may be an analog indication proportional to the number or rate of release of the photoelectrons. Interpreting this response in terms of photometric units requires a knowledge of the spectral quantum efficiency of the photomultiplier cathode and the spectral composition of the light being measured.

When the cathode of a multiplier is subjected to a small amount of light continuously, electrons will leave at a rate

$$n_e = \varkappa n_o$$

where n_o is the light flux in photons per second and $\varkappa$ is the quantum efficiency. The output from the phototube will consist of $\varkappa n_o$ pulses per second. These pulses will each have an average charge of eG where G is the multiplier gain. However, these pulses will not all be of the same size, but, because the secondary emission process is a statistical one, the pulse height will have a distribution.

It can be shown that, if n_e is the average number of photoelectrons in a pulse, the pulses from the multiplier will be distributed over a range of pulse heights having a nearly Gaussian distribution peak whose fractional width at half maximum (FWHM) will be given by

$$(\text{FWHM})_{n_e} = \frac{1}{\sqrt{n_e}} \frac{1}{\sqrt{\delta_1}} (1 + E/\delta - 1)^{1/2}$$

where δ_1 is the gain of the first dynode, δ is the gain of the remaining dynodes, and E an experimental coefficient with a value around 1.6. In particular, where the output pulse is the result of a single electron,

$$\text{FWHM} = \frac{1}{\sqrt{\delta_1}} (1 + E/\delta - 1)^{1/2}$$

With the conventional multiplier the pulse height distribution for single electrons is quite broad, since $\delta_1 \sim 5$, extending from zero pulse height to a value several times the height corresponding to eG. This is sketched in Fig. 15(a). With the multipliers having the first dynode of

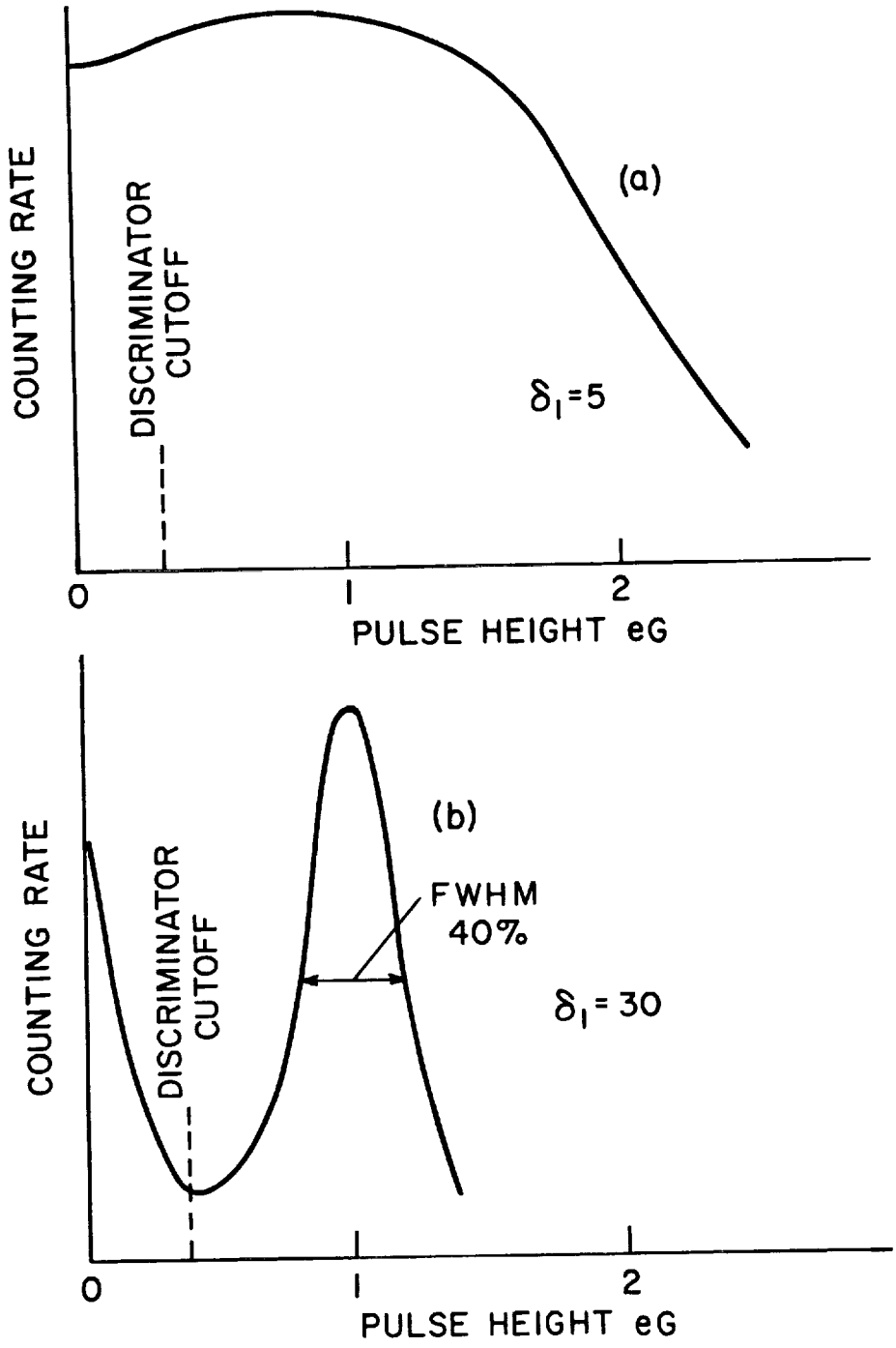

FIG. 15. PULSE-HEIGHT RESOLUTION. (a) CONVENTIONAL (b) HIGH-GAIN 1st DYNODE PHOTOMULTIPLIER

GaP (it is relatively unimportant what materials are used for the other dynodes of the chain) with a high gain, the distribution is much narrower. The pulse height distribution of this new multiplier with $\delta_1 = \sim 30$ for single electrons is shown in Fig. 15(b). It will be seen that the FWHM is only about 50% of its average pulse height (peak of the distribution).

When analyzing the pulse output from a photomultiplier, it is found that there is a high pulse rate of very small pulses - pulses whose amplitudes are quite small compared with eG. These are due to the coupling circuit between multiplier and amplifier, the amplifier itself, and certain non-fundamental processes in the multiplier. In order to avoid counting these pulses, a discriminator which rejects all pulses less than some preassigned height is used. Rejection of all pulses less than 1/3 eG gives close to optimum signal-to-noise ratio.

Where a conventional multiplier is used, the discriminator rejects a significant fraction of signal pulses from the single electron pulse height spectrum. If this fraction were constant, it would only be harmful to the extent it reduced the signal-to-noise ratio of the measurement. However, if the gain of the multiplier changes, the fraction of signal electrons lost is changed so that the absolute calibration of the measurement is lost.

With the GaP first-dynode multiplier, the single electron spectrum is sharp enough so that virtually no single electrons pulses are rejected by the discriminator. This being so, a relatively small decrease in gain due to fatiguing does not change the rate of signal electron pulses observed at the output. Therefore, the calibration in terms of pulses per second produced by n lumens of a given spectral quiality incident on the cathode does not change.

For photometry, it is probable that a literal counting of photoelectrons, like nuclear particle counting, is not the most desirable type of display. An analog reading proportional to the rate of occurrence of photoelectron pulses averaged over some predetermined time is more satisfactory. The averaging time can range anywhere from a fraction of a second to several seconds or longer, depending upon application requirements such as minimum light, accuracy requirements, and speed of response.

One of the simplest ways of carrying out this type of display or presentation is illustrated in Fig. 16. The multiplier is followed by a discriminator A which rejects all pulses below 1/3 eG and those above 1-1/2 eG. The pulse output from this single channel selector is supplied to a bistable (flip-flop) circuit B which is triggered by pulses of the height range of those passed by the discriminator. Each time this circuit

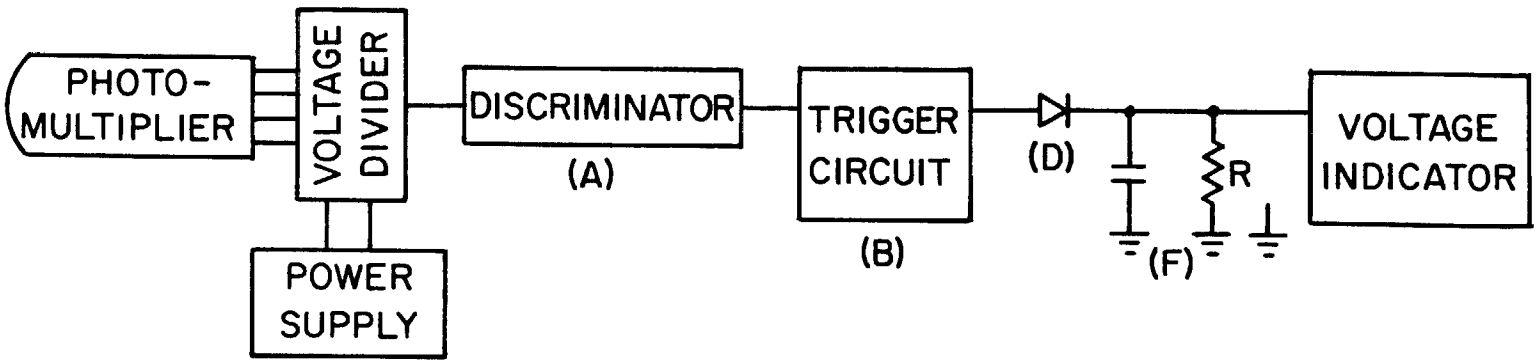

FIG. 16. PHOTON COUNTING

changes its state, it delivers a constant charge pulse through the diode D to the resistor-condenser combination F. The recorder or output meter G measures the voltage across the condenser. This voltage is proportional to the rate of photoelectrons n_e since, under steady state conditions, the condenser will reach a voltage where the average current into it $i_a = n_e q$ will just equal the current out through the resistor R. Thus,

$$V = i_a R = n_o(R_q)$$

The averaging time for such a system is t = RC. After almost any change in light level, the output meter will be in quite good equilibrium (1%) in a period of four to five time constants.

All the techniques used in the above type of presentation have been developed to a high degree of perfection in the nuclear physics field. Discriminator and flip-flop circuits can be built to respons up to uniform counting rates of 10^7 pulses/sec and 10^6 for random pulses. The integrator-rate circuit will, in actual practice, probably be somewhat more complicated than the basic R-C circuit outlined in order to increase its accuracy over a wide range of readings and to reduce time lost in simple exponential averaging. However, it presents no serious problem.

If it is assumed that one second averaging is used, then at a maximum counting rate of 10^6 per second, the rms deviation will be about 0.1%. It increases as the counting rate decreases and becomes about 3% at 100 per second.

At the maximum rate with 10^6 photoelectrons per second and assuming a quantum efficiency of 0.1 for the cathode, the incident light on the cathode will be on the order of 10^{-9} lumens. If at least 1% accuracy is required, the dynamic range is 100; that is, down to 10^{-11} lumens. This is very small for many photometric problems.

Still retaining the advantages of the photon counting method but increasing the dynamic range, a system of apertures, reflectors, or filters can be used to attenuate the incident light. As an example, the attenuator might be a pair of tapered filter disks,turned by a feedback servo in opposite directions, each being tapered in opposite sense. With well-calibrated filter disks, 1% accuracy should be achievable over a wide dynamic range.

If the spectral range of the light is not very large, an electro-optical (e.g., Kerr effect) shutter may be used to avoide the difficulty of a mechanical system.

VI. FEEDBACK STABILIZATION

Calibration for photometry can be stabilized for a multiplier which fatigues by the use of a feedback system. The feedback serves to hold the signal from a monitoring light source constant by controlling the over-all voltage applied to the multiplier.

This system does not give quite as much accuracy or sensitivity as the photon counting method but gives a large dynamic range without the need of a mechanical shutter. Its accuracy is compromised by requiring two standards, one a light source, the second a voltage or current against which to compare the multiplier output.

The system is closely related to that used to control the photocurrent in the fatigue-measuring unit used in the course of this contract. It employs a standard solid-state light source pulsed at 2000 cycles so mounted that it can be seen by the multiplier cathode but interfere as little as possible with the optical path for the light to be measured. This calibrating light is switched on every few seconds, for example, at 5-second intervals, for a brief period, e.g., 0.2 sec. During the active period, the 2000-cycle output is selected out of the signal, compared with a standard voltage, and the error signal used to increase or decrease the over-all multiplier voltage by controlling the regulator circuit of the multiplier power supply.

A block diagram of the system is shown in Fig. 17. The circuits for selecting the standardizing signal and for regulating the power supply are shown in Figs. 18 and 19. The greatest problem of this type of feedback is that of the light source. The most desirable type is a forward biased GaP diode. They are, however, very new and, while they reportedly hold their constancy quite well, their full performance capabilities are not known. A cathode ray light source is an acceptable alternative.

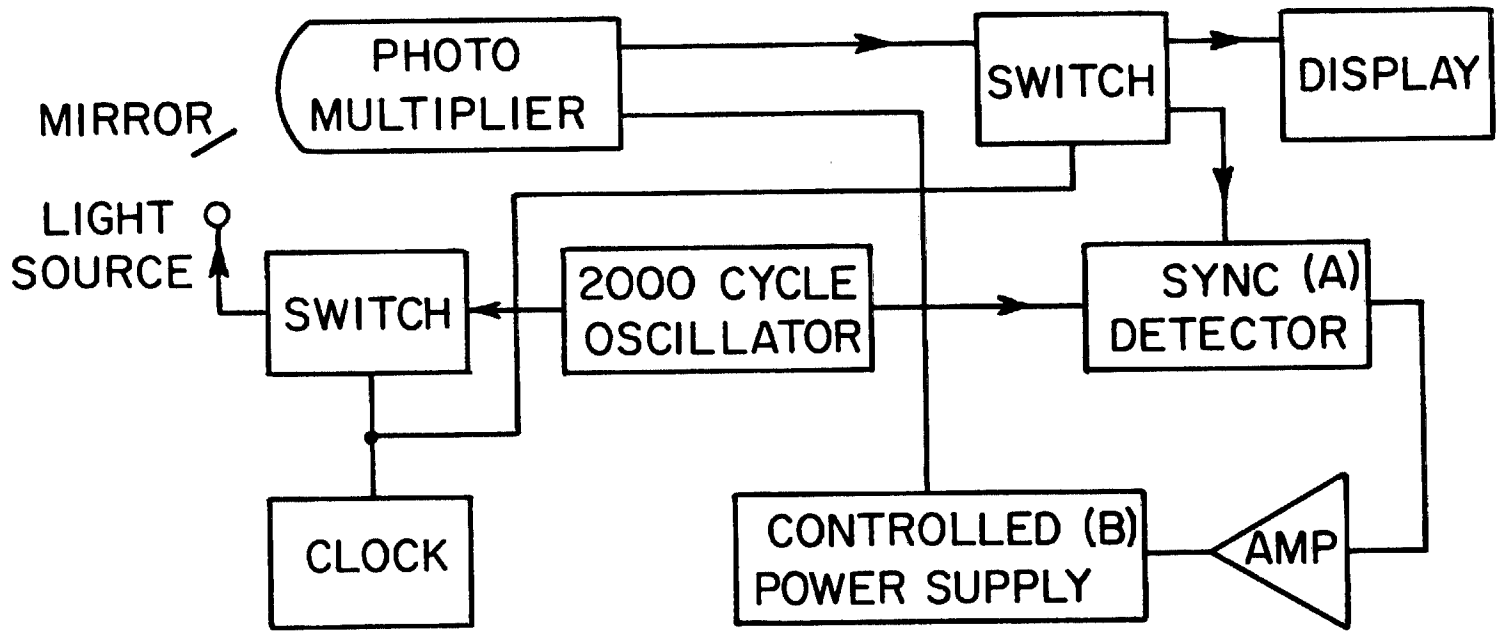

FIG. 17. FEEDBACK GAIN STABILIZATION

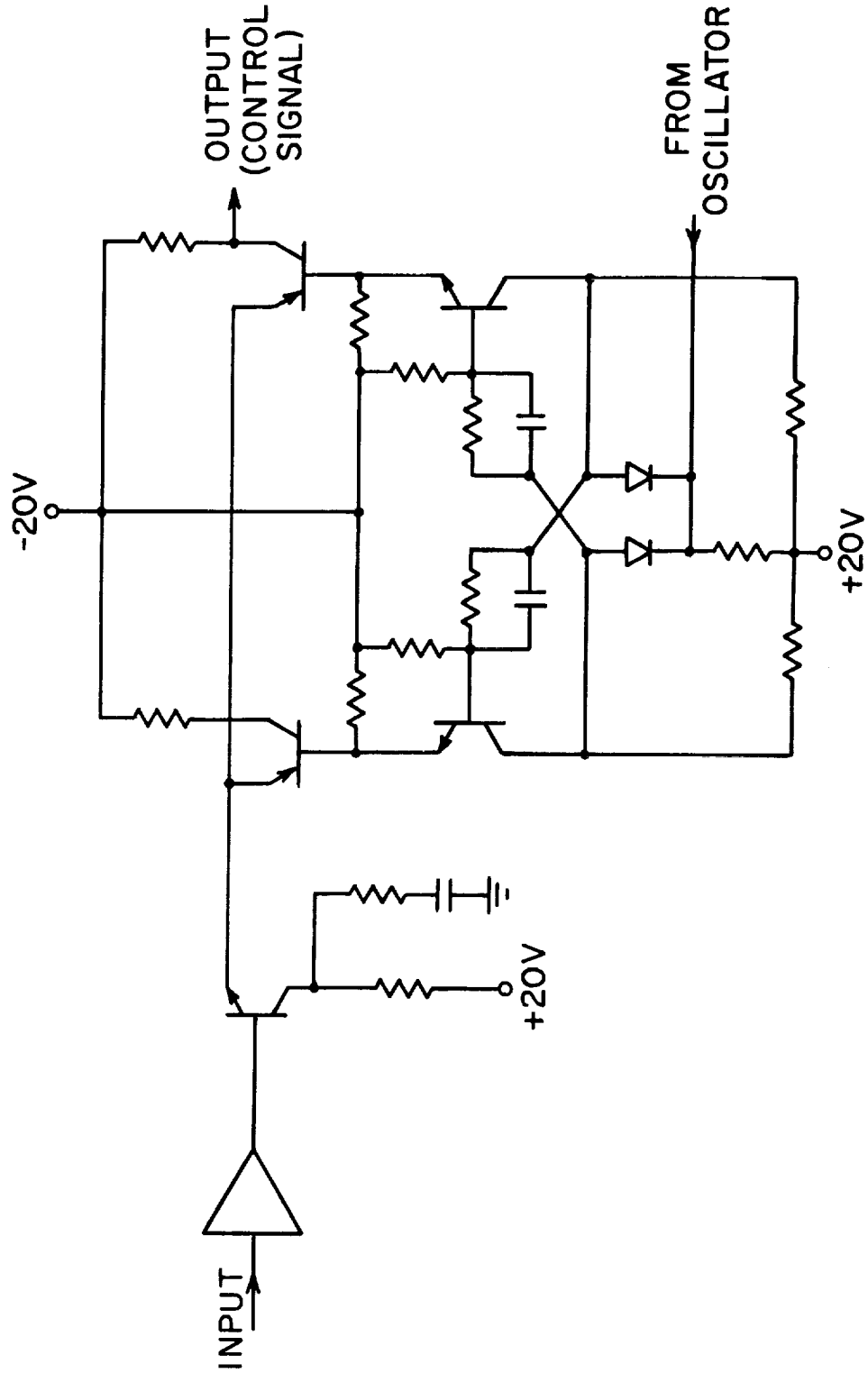

FIG. 18. DETECTOR FOR CONTROL CIRCUIT

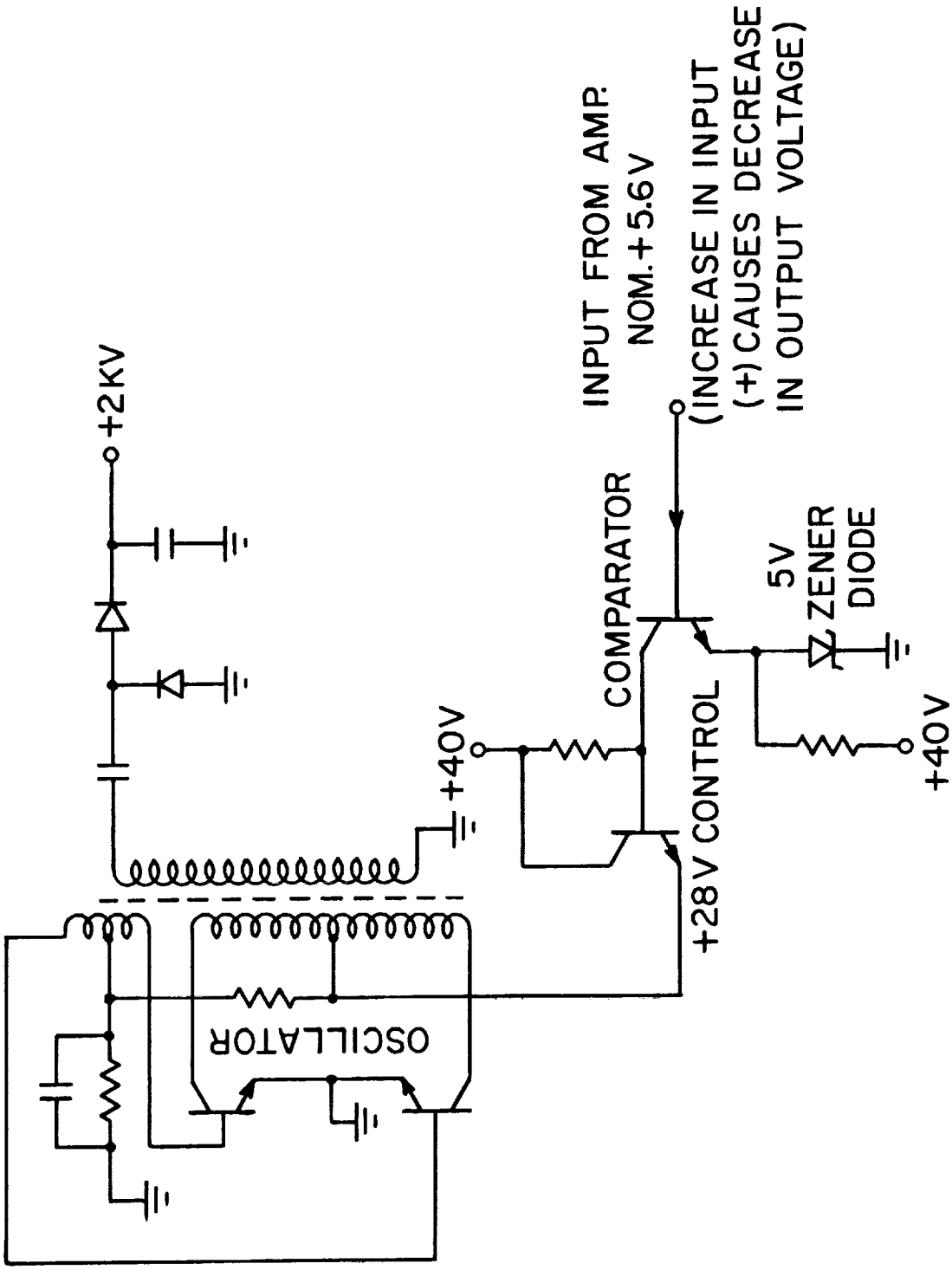

FIG. 19. CONTROLLED POWER SUPPLY

VII. CONCLUSIONS

The investigation of fatigue in conventional multipliers showed that the use of argon would not reduce the effect nor would operation in a low-voltage low-stage-gain mode. It was shown that a recovery process occurs which, after prolonged operation at a given output current, will lead to fairly stable operation at an average current equal to the aging current.

Most of the phase of the investigation covered by this report centered around the new GaP negative electron affinity secondary emitter. Four samples were studied in some detail. All exhibited very similar fatigue characteristics. It was shown that the fatigue was not only the result of surface changes which reduced electron escape probabilities but also included change in the effective depth from which excited electrons could reach the surface and be emitted.

The high-gain GaP dynodes showed recovery effects similar to those observed in conventional dynodes; however, recovery to the very high gains characteristic of newly activated GaP was not observable.

No method of overcoming the phenomenon of fatigue, either by surface treatment or by type of surface, was discovered.

Two circuit means of compensating fatigue in photomultipliers used in photometry are suggested. The first takes advantage of the very good pulse height resolution characteristic of the new photomultipliers using GaP dynodes for photon counting. Photon counting leads to a photometer which gives the greatest sensitivity possible with a multiplier having a given photocathode. The dynamic range obtainable with photon counting is normally limited because of circuit considerations. It can be greatly increased by the use of an electrically controlled (feedback) light attenuator in front of the photomultiplier.

The second form of photometer employs a standard light source giving (at suitable intervals) a calibrating signal which can be held constant by a feedback control of the photomultiplier voltage supply.

REFERENCES

1. Simon, R. E.; Sommer, A. H.; Tietjen, J. J.; and Williams, B. F.: New High-Gain Dynode for Photomultipliers. Applied Physics Letters, vol. 13, no. 10, 15 Nov. 1968, p. 355.

2. Morton, G. A.; Smith, H. M.; and Krall, H. R.: The Performance of High-Gain First-Dynode Photomultipliers. IEEE Transactions on Nuclear Science, vol. NS-16, no. 1, 1969, p. 92.

3. Cathey, L.: Fatigue in Photomultipliers. IRE Transactions on Nuclear Science, vol. NS-5, no. 3, December 1958, p. 109.

4. Engstrom, R. W.: RCA Technical Manual PT-60, 1963, pp. 67-69.

5. Bruining, H.: Physics and Applications of Secondary Emission. McGraw-Hill Book Co., Inc. 1954.

6. Dekker, A. J.: Secondary Electron Emission. Solid State Physics, vol. 6, 1958, p. 251.

7. Simon, R. E.; and Williams, B. F.: Secondary-Electron Emission, IEEE Transactions on Nuclear Science, vol. NS-15, no. 3, June 1968, p. 167.

8. Feldman, C.: Range of 1-10 keV Electrons in Solids. Physical Review, vol. 117, 1960, p. 455.

9. Seraphin, B. O.; and Bennett, H. E.: Semiconductors and Semimetals, vol. 3. (Edited by Willardson, R. K.; and Beer, A. C.). Academic Press, 1967.

10. Morton, G. A.: Photon Counting. Journal of Applied Optics, vol. 7, no. 1, January 1968, p. 1.

APPENDIX

As has been discussed in Section II, the general equation

$$S = \frac{B_s E L_s}{\epsilon R} (1 - e^{-R/L_s}) \qquad (1A)$$

where $R = AE^{1.35}$ $A = 1710$ $\epsilon = 8.7$

seems to apply fairly well to most secondary emitters. In the discussion, physical significance is given to B_s and L_s as being the surface escape probability and escape depth, respectively. These two values can be related to the photoelectric escape depth L_p and escape probability B_p. In order to obtain a better understanding of the processes occurring during fatigue, wherever possible B and L are determined from measurement of photoemission and secondary emission ratio S vs primary electron voltage.

In order to calculate the optimum B_s and L_s from the measured secondary emission values, the computer program reproduced in Fig. A-1 was used. The first part of this program tabulates the squared difference between experimental points and corresponding points obtained from Eq. (1A) for a selected B_s and a series of values for L_s. The minimum difference is the best fit. Initially B_s is selected from the slope of the S vs V curve near zero volts. Before naming the final L_s and B_s values, usually several values of B which bracket the value obtained from the slope measurement are tested to make sure that the B and L selected are the minimum for the two-dimensional field of B_s and L_s. This method of finding the optimum values was selected rather than programming the computer to give the minimum because it gives the operator a much better grasp of the physical situation.

Once the B_s and L_s have been selected, the second part of the program gives the data needed to plot the general secondary emission curve.

Comparison of experimental data points and the calculated curve is illustrated in Fig. A-2 for the pre-fatigue measurement on gallium phosphide sample E. In general, this is representative of the fit achieved.

Just as B and L for secondary emission can be evaluated from the type of data obtained, the corresponding values for photoemission can be found from the behavior of the spectral response near the long wave

```
 10 REAL B,A,V(15),L(51),T(15),X1(15),X2(15),S(31,15),D(51)
 20 99 READ A,F,M
 30 PAUSE
 40 DØ2 J=1,M
 50  READ V(J),T(J)
 60 2CØNTINUE
 70 PAUSE
 80 GØ TØ 103
 90 102 REWINDØ6
100 DØ3 J=1,M
110 READ(06,1004)V(J),T(J)
120 3CØNTINUE
130 103 READ B
140 DØ5 N=1,30
150 L(N)=200+10*N
160 DØ6 J=1,M
170 X1(J)=A*(V(J)**1.35/L(N))
180 IF(X1(J).GT.10.) X1(J)=10.
190 X2(J)=1-EXP(-X1(J))
200 S(N,J)=
    B*L(N)*(V(J)**(-.35))*X2(J)/(A*F)
210 6CØNTINUE
220 5CØNTINUE
230 DØ7 N=1,30
240 D(N)=0
250 DØ8 J=1,M
260 D(N)=D(N)+(T(J)-S(N,J))**2
270 8CØNTINUE
280 7CØNTINUE
290 101FØRMAT(5XF7.0,5XE15.6)
300 PRINT101 (L(N),D(N),N=1,30)
310 PAUSE
320 GØ TØ 103
330 PAUSE
340 READ K
350 DØ 89 J=1,M
360 PDUMP S(K,J)
370 89 CØNTINUE
380 PAUSE
390 REWINDØ6
400 DØ90 J=1,M
410 WRITE(06,1004) V(J),T(J)
420 90 CØNTINUE
430 1004 FØRMAT(F12.4)
440 EDIT
```

FIG. A-1. PROGRAM TO CALCULATE OPTIMUM B_s AND L_s FROM MEASURED SECONDARY EMISSION VALUES

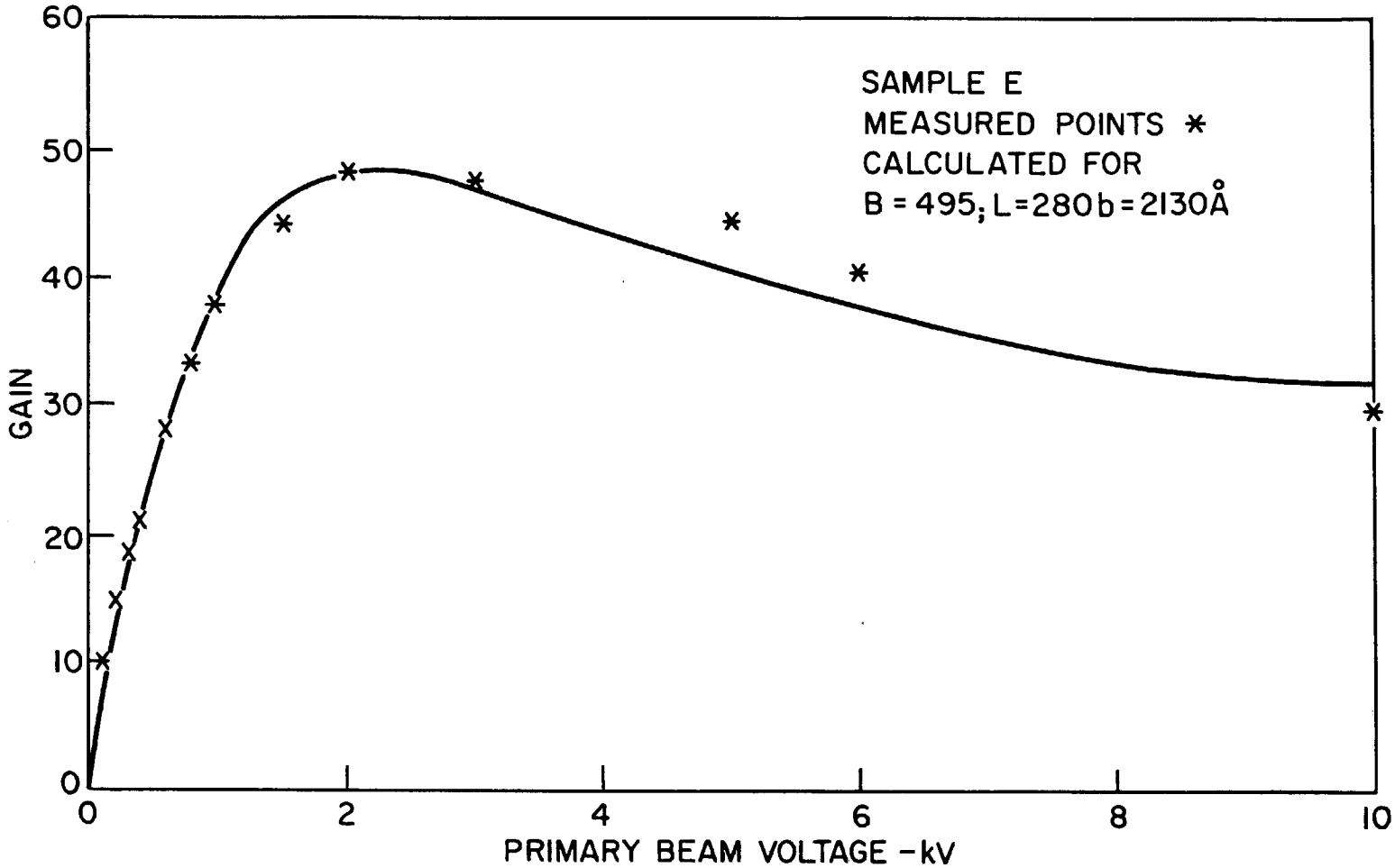

FIG. A-2. SAMPLE E GAIN VS VOLTAGE

threshold. It can be shown that the photoemission data can be represented by the curve

$$Y = A + Mx \tag{2A}$$

where

Y = (1 - reflectivity)/photoelectric quantum efficiency

A = 1/emission probability B_p

$M = 1/B_pL_p$

x = (absorption coefficient)$^{-1}$, the absorption coefficient being a known function of wavelength for GaP.

The program shown in Fig. A-3 was used to calculate the best slope and intercept of the line in Eq. (2A) using the correlation coefficient maximum as the measure of the best fit. The relative error rather than the absolute difference between data points and the curve representing them was used because of the wide range of values involved. The reflectivity R and the absorption coefficient α are quite well known for GaP. Values used in these calculations are given in the following table.

λ	$h\nu$	α	R
3536	3.50	4.0×10^5	.47
3640	3.40	2.95×10^5	.44
3751	3.30	1.75×10^5	.41
3868	3.20	1.00×10^5	.38
3993	3.10	7.15×10^4	.35
4126	3.00	5.40×10^4	.335
4268	2.90	4.10×10^4	.325
4421	2.80	2.40×10^4	.315
4587	2.70	3.60×10^3	.303
4761	2.60	1.50×10^3	.295
4951	2.50	6.3×10^2	.290
5157	2.40	2.66×10^2	.283

Values for the photoelectric quantum efficiency were obtained by comparing the response of the dynode with that of a standard phototube whose

```
  10  9 CONTINUE
  20  REAL LR
  30  COMMON X(101),Y(101),R(101),YY(101),YI(101)
  40  REAL CPT,L
  50  READ N
  60  DO 3 J=1,N
  70  READ X(J),Y(J),R(J)
  80  3 CONTINUE
  90  PAUSE
 100  X1=0
 110  X2Y2=0
 120  X1Y2=0
 130  Y2Y=0
 140  X2=0
 150  XY=0
 160  Y1=0
 170  Y2=0
 180  X2Y=0
 190  X1Y=0
 200  Y1Y=0
 210  DO 40 J=1,N
 220  YY(J)=R(J)/Y(J)
 230  YI(J)=1./YY(J)
 240  40 CONTINUE
 250  DO 4 J=1,N
 260  X1Y=X1Y+X(J)/YY(J)
 270  X2Y2=X2Y2+(X(J)/YY(J))**2
 280  X1Y2=X1Y2+X(J)/(YY(J)**2)
 290  Y2Y=Y2Y+YY(J)**(-2)
 300  Y1Y=Y1Y+1./YY(J)
 310  X1=X1+X(J)
 320  X2=X2+X(J)**2
 330  XY=XY+X(J)*YY(J)
 340  Y1=Y1+YY(J)
 350  Y2=Y2+YY(J)**2
 360  4 CONTINUE
 370  X1=X1/N
 380  X2=X2/N
 390  Y1=Y1/N
 400  Y2=Y2/N
 410  XY=XY/N
 420  SLP=(XY-X1*Y1)/(X2-X1**2)
 430  CPT=Y1-SLP*X1
 440  RHO=(XY-X1*Y1)/(SQRT((X2-X1**2)*(Y2-Y1**2)))
```

FIG. A-3. PROGRAM TO CALCULATE THE COEFFICIENTS OF EQ. (2A)
Continued on page A6

```
450 B=1./CPT
460 L=CPT/SLP
470 XN=N
480 SLPR=(1.*X1Y/X1Y2-1.*Y1Y/Y2Y)/(X2Y2/X1Y2-X1Y2/Y2Y)
490 CPTR=1.*Y1Y/Y2Y-SLPR*X1Y2/Y2Y
500 BR=1./CPTR
510 LR=CPTR/SLPR
520 PDUMP  SLPR,CPTR,BR,LR
530 PDUMP  B,L,RH0,SLP,CPT
540 D0  30  J=1,N
560 30  C0NTINUE
570 PAUSE
580 G0  T0  9
590 :Y(10)=.0012
```

quantum efficiency was known. A Bausch and Lomb monochromator was used as the source of light for these measurements.

A typical plot of quantum efficiency vs reciprocal absorption coefficient is shown in Fig. A-4.

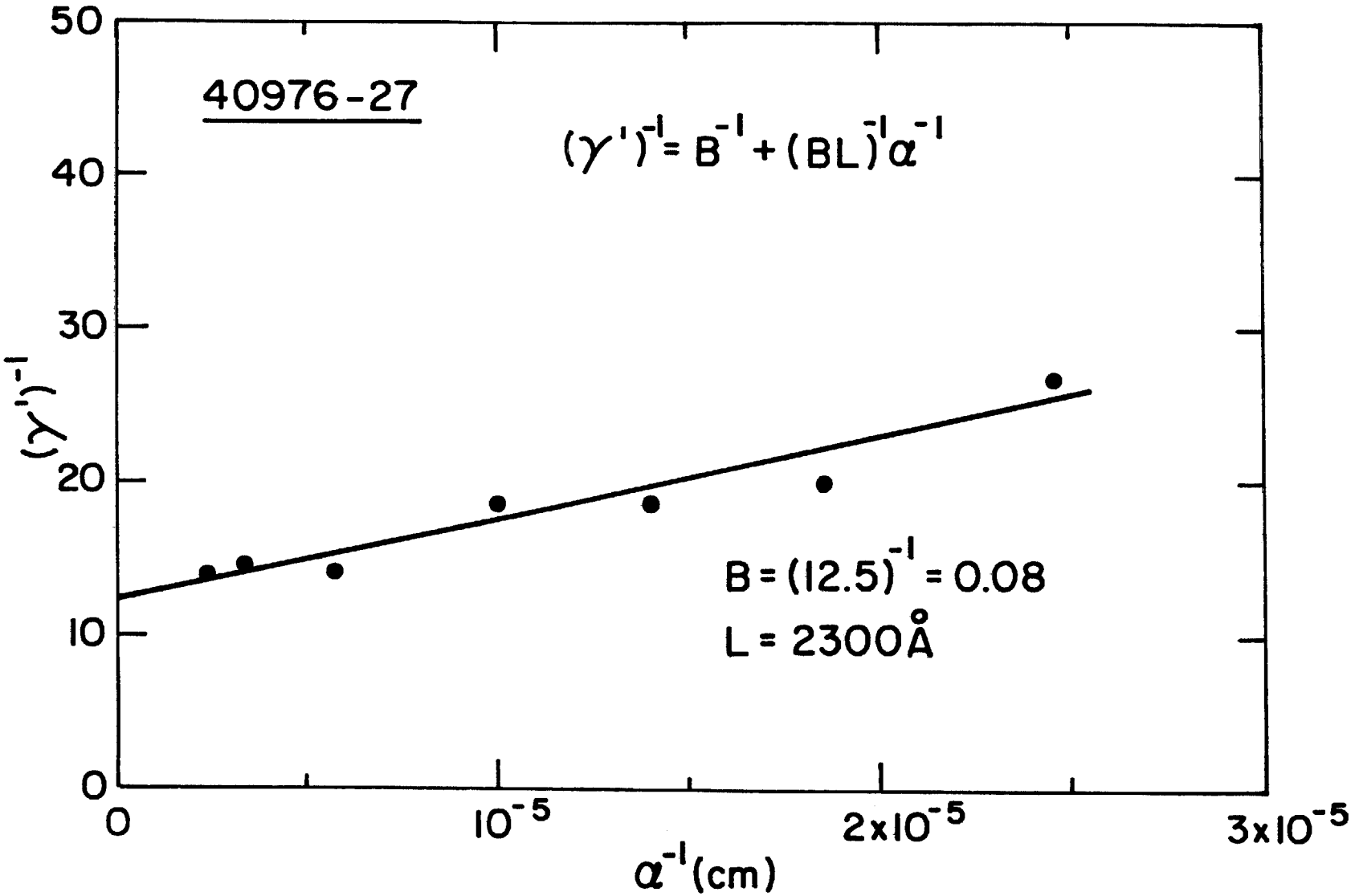

FIG. A-4. TYPICAL PHOTOELECTRON QUANTUM EFFICIENCY VS (ABSORPTION)$^{-1}$ CURVE

LIST OF SYMBOLS

A	Coefficient in primary electron range-energy relation
B	General surface escape factor
B_p	Surface escape factor for photoemission
B_s	Surface escape factor for secondary emission
C	Capacitance
D_n	Dynode n
E	Empirical coefficient in PMT pulse-height dispersion
E_p	Primary electron beam energy
E_K	Cathode potential
E_A	Energy of vacuum level below conduction band minimum
E_g	Semiconductor forbidden band gap energy
E(Cs-O)	Electron affinity of GaP:(Cs+O) surface
FWHM	Full width at half maximum of a PMT pulse height curve
f(x)	Secondary electron transport function
G	Overall PMT gain
ΔG	Change in overall PMT gain
h	Planck's constant, 6.62×10^{-34} joule-sec
i_A	Anode current
i_{D_n}	Current into dynode n
I_p	Primary current
I_r	Secondary current
L	Minority carrier diffusion length
L_p	Escape depth for photoelectrons
L_s	Escape depth for secondary electrons
N_e	Number of photoelectrons per flash of light
n_e	Number of photoelectrons
n_o	Number of photons
n	Exponent in primary electron ragne-energy relation
n(x,V)	Secondary electron distribution
Q or q	Electrical charge
R	Primary electron range

R	Resistance
R	Optical reflectivity of GaP
t	Time
V	Primary electron energy
$V_{o_{max}}$	Primary electron energy where secondary emission ratio is a maximum
x	Distance from vacuum surface into the dynode
Y	Spectral quantum efficiency
α	Optical absorption constant of GaP
δ	Secondary emission ratio
δ_n	Secondary emission ratio of dynode n
δ_{max}	Maximum value of the secondary emission ratio
ϵ	Energy required to produce a hole-electron pair
η	Quantum efficiency of the photocathode
ν	Frequency of radiation